DCT 216

Risk Analysis of a Scrap Tire Embankment

By

NII ATTOH-OKINE
OLUFIKAYO OLUWASEUN ADERINLEWO

Department of Civil and Environmental Engineering
College of Engineering
University of Delaware

September 2011

Delaware Center for Transportation
University of Delaware
355 DuPont Hall
Newark, Delaware 19716
(302) 831-1446

The Delaware Center for Transportation is a university-wide multi-disciplinary research unit reporting to the Chair of the Department of Civil and Environmental Engineering, and is co-sponsored by the University of Delaware and the Delaware Department of Transportation.

DCT Staff

Ardeshir Faghri
Director

Jerome Lewis
Associate Director

Ellen Pletz
Assistant to the Director

Earl "Rusty" Lee
T^2 Program Coordinator

Matheu Carter
T^2 Engineer

Sandra Wolfe
Event Coordinator

DCT Policy Council

Natalie Barnhart, Co-Chair
Chief Engineer, Delaware Department of Transportation

Babatunde Ogunnaike, Co-Chair
Dean, College of Engineering

Delaware General Assembly Member
Chair, Senate Highways & Transportation Committee

Delaware General Assembly Member
Chair, House of Representatives Transportation/Land Use & Infrastructure Committee

Ajay Prasad
Professor, Department of Mechanical Engineering

Harry Shenton
Chair, Civil and Environmental Engineering

Michael Strange
Director of Planning, Delaware Department of Transportation

Ralph Reeb
Planning Division, Delaware Department of Transportation

Stephen Kingsberry
Executive Director, Delaware Transit Corporation

Shannon Marchman
Representative of the Director of the Delaware Development Office

James Johnson
Executive Director, Delaware River & Bay Authority

Holly Rybinski
Project Manager-Transportation, AECOM

Delaware Center for Transportation
University of Delaware
Newark, DE 19716
(302) 831-1446

RISK ANALYSIS OF A SCRAP TIRE EMBANKMENT

ADERINLEWO OLUFIKAYO OLUWASEUN
ATTOH-OKINE NII

ABSTRACT

Scrap tires possess several advantageous properties which make them preferable to other materials as fills for embankment construction. Such properties include lightweight (the dry unit weight is 1/3 that of soils), high hydraulic conductivity (up to 23.5 cm/s) and low thermal conductivity. These properties of scrap tire fills results in low lateral pressures on the abutment wall and indirectly in reduced design and construction costs. The low thermal conductivity helps to prevent permafrost action of soil layers beneath it and failure of the subgrade due to frost penetration.

However scrap tires possess high compressibility, a property that leads to settlement of the fill and consequent failure of the embankment. Other undesirable attributes of scrap tire embankments are susceptibility to internal heating and leaching of substances into surrounding water.

An efficient means of controlling such undesirable attributes in the field is by comparing them with those simulated from a model embankment (the limiting criteria) developed by using Bayesian influence diagrams. In this work, the essential responses simulated by using analytica® software program are the temperature, lateral pressure, settlements and leachate characteristics. The most critical embankment characteristics, based on the maximum probability densities, are the settlement and horizontal pressures which are considerably low at 0.428 and 0.0034 respectively. Temperature response was not considered critical because the maximum probability density simulated was 0.9301. Limits for leachate concentrations were also obtained for the model embankment based on ASTM D 6270 (1998) standards.

TABLE OF CONTENTS

LIST OF TABLES

LIST OF FIGURES

LIST OF SYMBOLS

$\bigcap$ or X	-	intersection
$\bigcup$	-	union
ψ	-	clique potential
ϕ	-	separator potential
$\prod$	-	sum of the products of variables
$\sum_{Y}$	-	marginal sum of Y
$\sum_{Y \setminus X}$	-	marginal sum of X over Y
$\in$	-	is a member
H_{ct}	-	heat conductivity of tires
H_{cs}	-	heat conductivity of soils
Li	-	layer increment
H_l	-	heat liberated
Cov(X,Y)	-	rate of transfer
$\in$	-	belongs to
H_{ct}	-	heat conductivity of tires
Tphr	-	temperature per hour
C_c	-	compressibility coefficient
S	-	settlement
R	-	radius of application of load
σ	-	apply stress
P_p	-	passive pressure
K_p	-	coefficient of passive pressure
P_a	-	active pressure
K_a	-	coefficient of active pressure
γ_s	-	unit weight of sand
γ_{t1}	-	unit weight of top tire layer
γ_{t2}	-	unit weight of bottom tire layer
γ_w	-	unit weight of water
h_w	-	head of water
$P(X\|f)$	-	probability of X given f

Chapter 1: Introduction

1.1 Background

A number of alternative materials to soil have been considered in recent time for the construction of embankments such as fly ash, cement kiln dust, high-quality wood waste, construction and demolition debris. Presently, scrap tires are generating a lot of interest due to their versatility as construction material and useful properties such as high permeability, low thermal conductivity and lightweight. However, accompanying these favorable properties are three major disadvantages namely its large settlements, potential for internal heating and leachate effects.

In order to be able to predict and forestall failure of such embankments, it is necessary to be able to simulate the behavior of the embankment based on the loading and exposure conditions. The response of the embankment can then be varied using a software program and compared with the actual system as well as standard specifications to detect any anomaly.

The typical embankment investigated is considered to support the pavement that provides access to the integral abutment bridge. An integral abutment bridge is simply a single or multiple span bridge having its superstructure cast integrally with its substructure. Hence, the entire bridge undergoes deformation as a whole such as expansion and contraction depending on the temperature conditions. This affects the kind of pressure that the embankment exerts on the wall abutment whether passive or active. In addition, the foundation soil is mainly silty clay which is highly compressive.

The embankment is 18 feet (5.49m) thick and is required to be constructed in three layers, two of the layers constituting the top and bottom layers comprise of tire shreds and the middle layer consists of normal soil. The top layer is 10 feet (3.05m) thick, the middle layer is 3 feet (0.915m) thick and the bottom layer is 5 feet (1.525m) thick. The reason for using tire shreds otherwise called tire derived aggregates (TDA) is because of its light weight and the resulting low lateral pressures it will exert. Both of these are desirable qualities in this case since the foundation soil is weak and low lateral pressure on the abutment wall is required. Other advantages of using tire shreds in embankment construction are its high permeability (which ensures that it drains water quickly) and low thermal conductivity (which allows it to be used as an insulating layer

against subgrade frost attack). The tire derived aggregate has a maximum dimension measured in any direction of 8 inches.

However, using tire shreds in the embankment has three major disadvantages namely its high compressibility, tendency for internal heating and the possibility of leaching into surrounding ground water. Its high compressibility may lead to considerable settlements in time while its tendency towards internal heating as a result of large temperatures variations within may lead to fires and subsequent failure of the embankment. High settlements with time in tire shred fills can be controlled if an initial surcharge is applied during and immediately after construction of the embankment such that extensive compaction of the fill is achieved prior to use. The time settlements that occur thereafter will then be very negligible.

Influence diagrams can be described as a network for representing the probabilistic relationships between the variables that constitute the system behavior (Shachter, 1992) in which case, the system is the embankment behavior. The nodes represent the variables which have different kinds of information stored in them such as chance, decisions and objectives. The arrows represent the causal relationship between the variables. Using influence diagrams makes the work easy because it provides a descriptive way of analyzing the uncertainty between the variables which is represented by a probability distribution over the states.

Influence diagrams can be used to analyze a problem so as to arrive at the best solution for it. It can be used to monitor the entire response of a system and simulate the likely occurrences possible if one or several of the factors are added, altered or removed. By so doing, a likely model that properly represents the working of the problem can be developed. The influence diagram shows the dependencies between data and the state of knowledge at a decision point and they enable the evaluation of the outcome under different scenarios (Hao, 2000).

1.2 Motivation

Presently, Delaware and Alaska are the only states without scrap tire management programs. According to the United States Environmental Protection Agency (2005), Delaware has no specific legislation concerning the disposal, recycling or reuse of scrap

tires even though it has one that regulates storage and maintenance of existing tire piles. State officials estimate that about 750,000 scrap tires are generated each year and there are about 2.5 million scrap tires stockpiled in Delaware alone.

This work intends to encourage the development of such a waste tire program which will enable recycling and reuse of waste tires in embankments with reduction in the level of associated risk.

1.3 Statement of the Problem

Conventional soil material that is used for construction of embankments is expensive and difficult to source. Hence, alternative materials to soil are considered and waste materials such as scrap tires form the major basis for these because of their availability and easy accessibility. However, recovering or recycling these materials for use in construction requires a considerable level of awareness of their properties and the limitations associated with their use. It is therefore mandatory that recycled materials must pass three requirements namely toxicity, engineering and economic requirements.

The economic requirement is readily met by the fact that scrap tires are readily available in the environment and can be easily processed into smaller sizes for construction purposes by shredding and cutting. As a result, the overall relative cost of scrap tires in shredded or chip form is lower or comparable to that of conventional stone aggregate. Also, in several cases, tire chips have been known to cost one-third the amount of stone aggregate for use in septic systems (Grimes et al, 2003).

The ability of processed tire waste to meet the other two requirements namely toxicity and engineering requirements has necessitated a lot of laboratory investigation and field research. Under the toxicity requirements, it is required that water containing leachates from scrap tires fills should meet the regulatory limits for substances (metals and inorganic). These limits are described as primary and secondary drinking water standards. The primary drinking water standards determine what levels of the substances can be allowed in drinking water while the secondary drinking standards determine what levels of the substances can be permitted in surface water sources which will not adversely affect their aesthetics. Studies carried out on leachates from scrap tire

embankments have shown that the metals considered were generally below the regulatory allowable limits.

Under the engineering requirement, the use of scrap tires in embankment construction is required to solve a number of design problems. One of such is reducing the settlements in the foundation in a case where it is located on weak soils and using conventional soil would be too heavy. The other is lowering the lateral pressure on adjoining structures since scrap tire is lightweight. In addition, it is required that temperatures within the embankments constructed with scrap tires should be kept at a minimum to prevent the occurrence of fires as a result of internal heating.

However, there are no standards with which the measured engineering characteristics can be compared and which will give a quick and accurate assessment of the performance of the embankment. This means that hitherto, the performance of scrap tire embankments in terms of its engineering properties has been measured subjectively. Hence, developing a model that can simulate the characteristics of a scrap tire embankment of varying geometry and composition based on the loading and exposure conditions will help to alleviate this problem. The simulated characteristics will act as the ideal responses any similar characteristics measured in the field should meet for safe performance.

The ability of the model to adequately predict the embankment performance will also help to further generate interest in the implementation and development of scrap tire legislation and programs in Delaware State.

1.4 Objectives

The objectives are to:

i). Identify issues and challenges concerning the use of recycled scrap tires in construction and embankments in particular

ii). Develop a model that simulates the critical response of a typical scrap tire embankment using influence diagrams

iii). Analyze similar embankments for risk by comparing characteristic data obtained from them using sensors with the responses generated by the model.

1.5 Research Approach

The process by which the performance of the embankment is analyzed involves developing a model that can simulate the characteristics of a typical embankment. This requires an understanding of the structural features and the underlying properties of the constituent materials.

The exposure conditions which include the types of loads the embankment will carry and the temperature conditions are built into the model. In addition, the results of previous experiments and specifications outlined in standards are also used to develop the model. The results from the model can then used to check the responses of any typical real life embankment.

1.6 Thesis Organization

The remainder of this report is divided into the following chapters; the literature review which defines scrap tires, identifies their properties, describes their mode of generation and the processes developed for managing them. It discusses various research work aimed at developing scrap tires into alternative construction materials and the limitations to their application in construction. The concept of influence diagrams as well as the algorithms for solving them and their applications is introduced and discussed.

Chapter three involves the development of the model for analyzing risk in the embankment using influence diagrams and a computer program. Chapter four covers the analysis of data obtained from chapter three and interpretation of the results. Chapter five consists of the conclusion and recommendations.

Chapter 2: Literature Review

2.1 Introduction

Scrap tires according to the American Society for Testing and Materials (ASTM 1998) can be defined as tires which can no longer be used for their original purpose due to wear or damage. The amount of scrap tires in the environment is disturbing and the number keeps increasing.

Presently over 281 million tires are discarded annually as scraps while more than 300 million scrap tires are currently in stock piles throughout the United States (Rubber Manufacturer's Association 2005). An estimate of approximately 50 million used tires are discarded annually into landfills (Garga and O'Shaugnessy 2000).Tire piling is dangerous because they provide a breeding ground for rodents and mosquitoes and are vulnerable to fire from arson, lightning and spontaneous combustion or self ignition while landfilling is becoming unacceptable because of the rapid depletion of available sites for disposal waste disposal. This has generated a lot of interest in developing new methods for dealing with the scrap tires.

One of the major steps in this direction is by utilizing the 4 R's namely reduce, re-use, recycle and recovery (Maryland Department of the Environment 2005). Reduction of the volume of scrap tires generated can be achieved by creating awareness in the public to use their tires in such a way that their longevity is prolonged and this will require gauging their tires regularly for correct pressure, re-use of scrap tires involves building them into artificial reefs and breakwaters by bundling the scrap tires together and then anchoring them in coastal waters or rethreading them for continued use, recycling involves grinding scrap tires into rubber crumbs which can be remolded into useful new products and recovery of scrap tires involves grinding them into smaller pieces to be used as fuel called Tire Derived Fuels (TDF) in solid fuel burners such as kilns and paper mills.

A tire comprises of rubber or polymer material strongly reinforced with synthetic fibres, high strength steel wire reinforcing bead and high strength steel (or fabric belts) which produces a material having unique properties such as very high tensile strength, flexibility, resiliency and high frictional resistance (Garga and O'Shaughnessy 2000). The beads consist of rubber covered metal wires or braids and the tire fabric is made of

braided rayon cord. Tires are able to withstand high stress levels imposed during soil compaction because they are able to deform to the same extent as the surrounding soil. The reported ignition and sometimes explosion of tire in fills has been a source of concern even though there has been no such report concerning recent earth fills constructed in accordance with new design guidelines which minimize internal heating. In order to set a tire containing structure on fire, a continuous and intense application of heat is required and only the exposed tires at the surface are normally burnt.

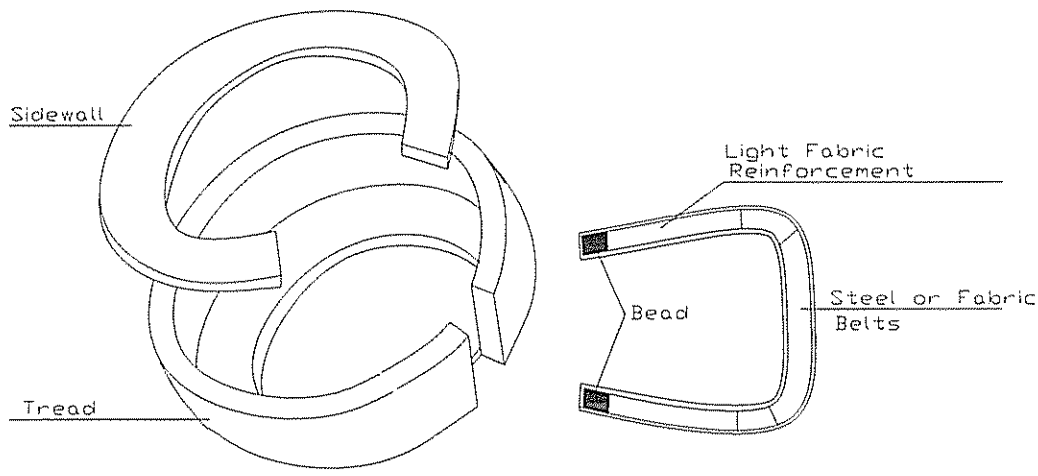

Fig 2.1. Components of a typical tire

The management of scrap tires involves their proper treatment and handling through adequate disposal methods and recycling processes such that they do not constitute a nuisance to the society. Scrap tires can be disposed of in landfills however this takes up a lot of space hence alternative disposal methods and better still, reuse/recycling methods need to be developed that will be energy efficient, economical ,beneficial and capable of utilizing large quantities of it. Twenty-five states have banned the disposal of scrap tires in landfills entirely (Moo-Young et al 2003), nevertheless, a major part of the current scrap tire generation still ends up in landfills. Since the ban on

landfilling of whole tires was implemented in most states, scrap tires must now be cut into pieces or shredded before landfilling.

In December 1991, the United States Congress signed into law the Federal Intermodel Surface Transportation Efficiency Act requiring that 5% of all federally funded roads laid iun 1994 must contain scrap rubber from tires (Cecich et al 1996).This resulted in more rubberized roadways being laid in the United States since 1991. In addition, scrap tire management regulations/legislations have been established since year 2000 in 48 states out of the 50 United States while 12 states have banned all forms of scrap-tires from being disposed off in landfills (Siddique and Naik 2004).Table 1 shows facts and figures concerning scrap tires in the United States.

Table 2.1 Some facts and figures concerning scrap tires in USA (Rubber Manufacturer's Association, 2005)

Facts	Figures
Number of scrap-tires generated annually	281 million
Approximate weight of scrap-tires	5.68 million tons
Number of scrap-tires in stock piles	300 million
Number of tires processing facilities	498
Scrap-tires used in civil engineering applications	40 million
Scrap-tires processed into ground rubber	33 million
Scrap-tires used for fuel	115 million
Number of scrap tires exported	15 million
Number of states with scrap-tires legislation/ regulations	48
Number of states that ban whole tires from landfills	38
Number of states that ban all scrap-tires from landfills	11
Number of states with no landfill restrictions	8

In the State of Delaware, about 780,000 scrap tires are generated each year and there are currently 38 known stockpiles. The hazards these stockpiles can lead to could best be imagined. Hence, Delaware Center for Transportation (DCT) researchers are collaborating with the Delaware Department of Transportation (DELDOT) to develop a

scrap tire program for Delaware. The program will be responsible for managing all Delaware systems and activities concerned with collecting, storing, recycling and processing scrap tires.

Scrap tires can also be disposed through the process of devulcanization which involves breaking the sulfur bonds that hold vulcanized rubber in shape, a characteristic that also prevents the possibility of melting tires down and remolding them into new products. There are several variations of devulcanization namely Thermal, Mechanical, Bacterial and ultrasound devulcanization. Thermal devulcanization involves exposing rubber to high temperatures for an extended period of time to break the sulphur bonds. The process also breaks the polymer chains themselves, severely degrading the value of the rubber. It presents environmental and public health risks and is rarely used today. Mechanical devulcanization uses rollers, mixers and extruders to mechanically break down the sulfur bonds. It produces good results but is not yet economically viable. Bacterial devulcanization involves grinding rubber to a powder and suspending it in a liquid full of sulfur-eating bacteria such as thilbacillus, rodococcus and sulfolobus. The process is technically viable but complex, and therefore too expensive. However, the devulcanization of scrap tires using ultrasound technique produced encouraging results even though it is also expensive.

Theophillic microorganisms have also been used to devulcanize (biodesulurize) the surface of ground rubber particles which improves the bonding and adhesion of ground rubber tires into virgin tire rubber matrix which can be used to improve asphaltic materials, rubber and polymeric wastes as well as enable their recycling (Maryland Department of the Environment 2005).

Alternatively, scrap tires can be recycled by grinding them into rubber which can be used for making new products such as floor mats, carpets and plastic products. They can also be processed into smaller pieces for use in civil engineering applications. Presently, 10 million scrap tires are recycled into new products, 33 million are processed into ground rubber, 115 million are used as fuels and 40 million in civil engineering applications (Rubber Manufacturers Association, 2005).The fuels are produced by burning the tires whole or in shredded form (that is, chunks), hence they are called tire

derived (TDF). Burning whole tires saves the cost of shredding but could increase the cost of transportation and storage.

TDF's are used either entirely alone or in combination with other fuels in cement kilns, pulp and paper mills, electricity utilities, waste-to-energy plants and industrial boilers and they account for the largest single use of scrap tires. Pyrolysis, defined as the thermal distillation or decomposition of organic materials into oils, gases and char is another process by which tire-derived fuels are produced from scrap tires. Unfortunately, efforts to commercialize this technology have failed because it is not yet economically viable in the United States due to the fact that it requires expensive equipment as well as high operational and capital investment. In addition, the products of tire pyrolsis are low in quality hence they have limited selling appeal.

In the state of Maryland, three agencies were assigned the task of implementing a scrap tire program which involved collecting, transporting and recycling/processing of scrap tires. The agencies are the Maryland Department of the Environment (MDE), Maryland Environmental Service (MES) and the Comptroller of the Treasury. A $6 million grant was awarded by the Department of Health and Environmental Control (DHEC) to the City of Clemson and its partner, Clemson University to establish a research center that would develop new means for removing scrap tires from their state. These two partners were also required to investigate on how recycled tires could be introduced into the construction of highways, roads, embankments, retaining walls, running tracks, golf course cat paths and erosion resistant beach walls.

Scrap tires can be used wholly or they can be processed into smaller more manageable proportions namely slit, shredded or chipped tires, ground rubber and crumb rubber. Slit tires are produced in tire cutting machines that are capable of slitting a tire into two halves as well as separating the sidewalls from the thread of the tires. Tire shreds are also processed with knife cutters rotating at slow speed and their general sizes vary between 50mm and 305mm with most of the wire belt removed. The width of a shred depends on the knife spacing and the length can be as much as the diameter of the wire. Tire chips are much smaller varying between 12 and 50mm in size. Tire shreds are sized with the aid of a rotating screen called a trommel or a classifier comprising parallel bars spaced several centimeters apart. According to Siddique and Naik (1995), tire shreds are

produced through a primary process with sizes varying from as large as 300 to 460 mm long by 100 to 230 mm wide, down to as small as 100 to150 mm long depending on the manufacturer's shredder model and the condition of the cutting edges while tire chips are normally sized from 13 to 76 mm and produced by a combination of the primary and secondary processes.

Ground rubber is produced by grinding scrap tires (granulators, hammermills, or fine grinding machines) into regularly shaped spherical and cubical particles with a comparatively low surface area. They maybe be sized from particles as large as 19 mm to as fine as 0.15 mm (No. 100 sieve) depending on the type of size reduction equipment used and the intended application (Siddique and Naik 1995). The steel belt fragments are removed by a magnetic separator. Fiberglass belts or fibers are separated from the finer rubber particles in most cases by an air separator. Ground rubber particles are subjected to a dual cycle of magnetic separation, then screened and recovered in various size fractions.

Crumb rubber is produced by three methods. The most often used method is the cracker mill process which tears apart or reduces the size of tire rubber by passing the material between rotating corrugated steel drums. This process creates an irregularly shaped torn particle with a large surface area and ranging in size from approximately 5 mm to 0.5 mm (No. 4 to No. 40 sieve), hence, they are commonly referred to as ground crumb rubber. The second method is the granulator process, which shears apart the rubber with revolving steel plates that pass at close spacing thereby producing granulated crumb rubber particles ranging in size from 9.5 mm to 0.5 mm (No. 40 sieve). The third process is the micro-mill process, which produces a very fine ground crumb rubber in the size range from 0.5 mm (No. 40 sieve) to as small as 0.075 mm (No. 200 sieve).However, typical sizes of crumb rubber used vary from 4.75 mm (No. 4 sieve) to less than 0.075 mm (No. 200 sieve).

In some cases, cryogenic techniques are also used for size reduction. Essentially, this involves using liquid nitrogen to reduce the temperature of the rubber particles to minus 87° C (-125° F), making the particles quite brittle and easy to shatter into small particles. This technique is sometimes used before final grinding into crumb rubber.

2.2 Properties of scrap tires

Tire shreds and tire chips are terms generally used to describe scrap tires however this is an overgeneralization because scrap tires also include ground rubber and crumb rubber. Some of the desirable properties of tire shreds include their lightweight (6.4 to 9.6 kN/m^3), free draining or high permeability (greater than 10m/s), low earth pressure (50% at base of 16ft high wall) and unit weight, good thermal insulating (8 times better than gravel), high durability and inexpensiveness for many applications. Their use also consumes waste tires thereby reducing waste in the environment.

The three major disadvantages are large immediate settlements, settlements in time, potential for internal heating and leachate effects on surrounding ground water.

2.2.1 Physical and Chemical tests on recycled scrap tires and its composites

In order to identify the properties of scarp tires, the following physical tests namely water absorption, specific gravity, compaction, permeability or hydraulic conductivity, shear strength and compression tests were performed according to the American Society of Testing and Materials (ASTM) standards (1998). The chemical tests carried out included the pH, turbidity, total organic carbon and iron content according to the American Public Health Association (APHA) standard methods for the examination of water and wastewater (1999).

2.2.2 Specific gravity, water absorption and unit weight

Specific gravity is the ratio of the particle unit weight or unit weight of solid tire shreds to the unit weight of water while adsorption capacity is the amount of water absorbed onto the surface of particles expressed as the percentage of water based on the dry weight of the tire particles (Humphrey 1998). The specific gravity of tire shreds ranges from 1.02 to 1.36 depending on the amount of glass belting or steel wire in the tire (Edil et al 2004) Both of these parameters are determined in accordance with ASTM C 127.

Chu (1998) carried out experiments on three different sizes of scrap tires (7mm - 13mm, 13mm-25mm and 25mm-38mm sizes) mixed with either clay or silt soils to

determine their maximum dry densities. The results showed that for both soil- tire mixtures, increasing the tire shred content led to a decrease in the dry density. Furthermore, the maximum dry densities are reduced to 2/3 the values for soil alone at approximately 50% tire content indicating that a lightweight fill material can be produced by mixing 50% soil with 50% tire material by weight. The work also showed that a semi-lightweight fill can be produced at shredded tire content less than 50%. The optimum water content decreased only slightly from 15 and 16% for pure silt and clay soil to 14% at 50% shredded tire content. Thereafter, there was rapid decrease from 14% to less than 8% at 90% tire content for both soil types and the three tire sizes used.

Moo-Young et al (2003) performed water absorption and specific gravity tests on random samples of tires shreds obtained from Wind Gap, Philadelphia with size ranges between 50 and 300mm.The water absorption of the tire shreds ranged from 6.7 to 7.0% while the specific gravity of the shreds ranged from1.06 to 1.12 which are similar to the results from the works of other researchers. The reduced unit weight of scrap tires is the most often cited advantage of using scrap tires. The dry unit weight normally varies between 6.4kN/m^3 and 9.6kN/m^3 which is 1/3 that for soils. Hence, they are useful as lightweight fill for embankment and road bases. The low unit weight results in low vertical pressures and consequently, low horizontal pressures. Hence, they are also useful as backfill material for walls and bridge abutment. This way, thinner and less expensive walls can be constructed.

2.2.3 Compaction

Compaction is the process of reducing the pore spaces between the tire shreds under an applied stress or pressure thereby increasing the weight of solids per unit volume of soil. Moo-Young et aL (2003) performed compaction tests on tire chips and tire shreds using a 30.48 cm compaction mold with a modified compaction hammer and a 222N weight dropped 91.4 cm. The loose density of the shreds was determined by pouring the tire shreds into the compaction mold and weighing the mold. A standard Proctor compaction energy of 355 kJ/m^3 (60% of the compaction energy) was used which was later increased to 2693 kJ/m^3 (100% of the compaction energy). Increasing the

compaction energy during the laboratory compaction tests did not have any significant effect on the final compaction density.

2.2.4 Hydraulic conductivity (Permeability)

Hydraulic conductivity is defined as the ease with which the tire shreds permit water to move through its fiber matrix. It is measured using a constant head permeameter and typical values range between 0.58cm/s and 23.5cm/s. Scrap tires offer very high hydraulic conductivity to water. In most of the experiments performed by researchers, the hydraulic conductivity showed an increase as the tire shred sizes increased.

The permeability of soil-tire mixtures was found to increase by six orders of magnitude (10^{-7} to 10^{-2}cm/s) when the shredded tire content was increased from 10% to 40% for both the silt-tire and clay-tire mixtures and the three sizes of tire chips used. Beyond 40% tire content, the permeability of the mixtures increases only slightly from 10-2 to 10-1 cm/sec at 10% shredded tire content for both soil types and all three sizes of tire chips.

Experiments by Humphrey and Tweedie (2002) have shown that tire shreds possess hydraulic conductivities higher than 1cm/sec which promotes rapid drainage of water when it is used as backfill material. According to McKenzie (2003), scrap tires in tire chips form contain 62 percent void space, as compared to 44 percent with stone. This allows tire chips to hold more water than stone.

Cecich et al (1996) calculated the hydraulic conductivities of tire shreds to be between 0.033 to 0.034cms^{-1} which are comparable to sandy or gravelly soils. Moo-Young (2003) conducted tests on tire shreds to determine how their hydraulic conductivity changes as the particles size increases. The permeameter used had a diameter of 30.44cm and a height of 91.2cm.

2.2.5 Compressibility

Scrap tires have high compressibility and this is defined as a measure of the decrease in scrap tire volume under pressure or a measure of the amount of settlement in the scrap tire volume under pressure. This is adduced to their high level of porosity and rubber content.

Chu (1998) found out that compressive index values of soil-tire mixtures increased with increase in the shredded tire content in each soil-tire mixture. In fact, the index values for the two soil types (0.05 for silt soil and 0.10 for clay soil) are doubled at 30% shredded tire content for all three sizes of tire chips indicating that settlement will increase with increasing shredded tire content.

According to Yang et al (2002), small tire chips have much lower compressibility than large-sized tire shreds (100 to 900mm long) that exhibit 40 % vertical strain at a vertical applied stress of about 17kPa.The main reason for this is that the initial void ratio of large sized tire shreds was about 3 while the initial void ratio of small tire chips(ranging in size from 2 to 10mm) was 0.98.The second reason is that individual large shreds are more compressible than individual small chips unlike moist other particulate systems in which the solid phase is incompressible as compared with the deformations that result from particle movement.

Scrap tires compress when a load is applied primarily due to two mechanisms namely bending and orientation of the fibres into a more compact packing arrangement and compression of individual tire shreds under stress. The compressibility of tire shreds is important in the design of landfill final covers so as to be able to assess the settlement that occurs during construction and the settlement that occurs due to overlying protective vegetative layer. It can be measured by placing the tire shreds in containers that have diameters ranging from 150mm to 750mm and then measuring the vertical compression caused by an increasing vertical stress. Moo-Young et al (2003) conducted compressibility tests on scrap tires at various sizes and on tire shreds mixed with soil at different mix ratios in order to determine the following; settlement that occurs during construction in the first couple of months which would facilitate a proper design that would account for such settlement, deflections caused by live or temporary loads post-construction and the in-place unit weight of compressed scrap tire. The compressibility of scrap tires can also be measured in terms of the resilient modulus which is defined as the compressibility of tire shreds under a moving vehicle load (Humphrey 1998).

The compressibility of scrap tires is often cited as their main disadvantage for use in roadway embankments. Compressibility of tire shreds is divided into two components namely an initial time settlement immediately following loading and a secondary creep

settlement that occurs under constant loading. The creep settlement may continue long after the initial loading of the fill. The compressibility of tire shreds complicates two aspects of embankment construction namely the ability to obtain a final grade and the ability to obtain adequate compaction of overlying soil and pavement structures. These are resolved by delaying the paving process to allow the initial settlement of the fill to occur.

2.2.6 Shear Strength

The shear strength between two particles is the force that must be applied to cause a relative movement between the particles. Shear tests were also conducted by various researchers on scrap tires of various particle sizes by using a direct shear or triaxial shear apparatus.

Chu (1998) carried out unconfined compressive strength tests on silt-tire and clay-tire mixtures and found out that the unconfined compressive strengths decreased with an increase of shredded tire content for both soil types and all three size ranges of tire shreds used (7mm -13mm, 13mm-25mm and 25mm-38mm sizes). He also investigated two distinct parameters under the shear strength tests namely the friction angle and the cohesion. He discovered that the cohesion decreases with increasing tire content for both the silt-tire and clay-tire mixtures containing 7mm -13mm sized shredded tire material. In the case of the other two size ranges, the cohesion increases at 10% shredded tire content by weight and then drops. He also found out that the amount of shredded tire content in the soil-tire mixture should not exceed 20% for improved friction angle.

Yang et al (2002) showed that the shear strength of shredded tires is independent of particle size and that the variation in strength parameters depends on the normal stress at which the specimens were tested. The stress range of the tests as well as the criterion used to define the failure influence the Mohr-Coulomb parameters. The power function equation provided an empirical model for interpreting direct shear results over a wide range of normal stresses.

However, Moo-Young et al (2003) also conducted similar tests and showed that there was actually a relationship between the shear strength of scrap tires and their sizes. He discovered that as the particle size increased, the shear strength of the scrap tires also

increased. It is noteworthy that the highest shear strength parameters were achieved with particle sizes ranging from 50mm to 100mm. The minimum aspect ratio to the largest particle size considered was 2 to 1.The normal force applied to the specimen was 1334.5kN through the universal testing machine. A series of hydraulic jacks and power unit were used to shear the specimen. The shearing rate was maintained by adjusting the hydraulic pump and the shear force was read from the load cell. The shear strength of mixtures of sand/gravel and tire shreds have also been obtained and it increases with increase in rubber content (Ilker 1995).

2.2.7 Toughness and Ductility

Topcu (1995) measured the toughness of rubberized concrete by measuring the areas under the stress-strain diagrams of test specimens. Rubberized concrete produced more strain at the time of fracture because rubberized concrete absorbs more energy. The maximum strain values obtained from the stress-strain diagram can reach 0.007 to 0.008.Toughness values in terms of energy capacities consumed at the time of fracture were investigated in two different ways as plastic and elastic properties. The energy capacities are illustrated as shown in figure 2. The high elastic energy of normal concretes decreased with the addition of rubber and originally low plastic energy capacities begin to increase.

High plastic energies in concrete indicate that the concrete could show higher deformation at the time of fracture and it could absorb more energy, hence, concrete plastic energies can be increased by mixing rubber into it and it begins to show the behaviour of an elastic material under load.

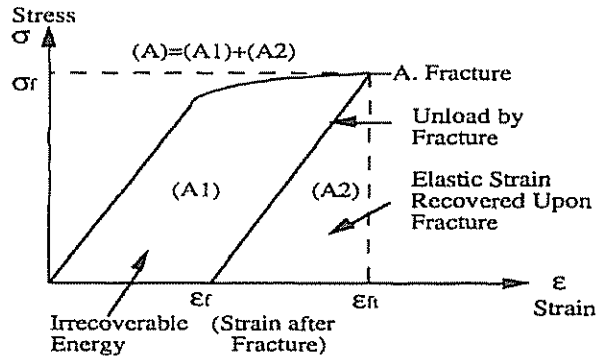

Fig. 2.2: Elastic and plastic energy capacities of rubberized concrete

Pierce and Blackwell (2002) observed an increase in the ductility of flowable fill specimens produced with crumb rubber (as an alternative to fine sand aggregate) under unconfined compression test. Stress-strain curves were compiled for the tests and they indicated that the compressive strength and the modulus of elasticity increased with curing time. The curves also showed that stress can be sustained to nearly 4% strain before fracture. This represents an increase in ductility when compared to standard flowable fill which achieved only 0.025 strain before fracture. This suggests that crumb rubber is an ideal aggregate for flowable fill even though the mass density and compressive strengths are reduced.

2.2.8 Thermal Conductivity

Scrap tires have very low thermal conductivities, about eight times lower than that of gravel (Humphrey 2002).The thermal conductivity of scrap tires increases as particle size increases, and more air can circulate in the voids. This way, the scrap tires become less effective as insulators. Lawrence et al (1999) showed that the thermal conductivity of tire shreds increased with particle size, increased water content and increased compaction. Also, thermal conductivity was higher for tire shreds tested under frozen conditions than under thawed conditions. Therefore, scrap tires with a maximum size of 75mm should be used for insulation projects because larger sized shreds will allow more air to circulate through the voids and this may lead to fires.

2.2.9 Chemical Tests

Moo-Young et al (2003) conducted pH, total organic carbon (TOC), turbidity and iron tests on effluent from the column test. The pH test on tire shreds gave a value of 6.98 indicating slight acidity.

The column test was carried out on the tire shreds using a 30.54cm diameter by 91.44cm high column made from clear polyvinyl chloride (PVC). Rainwater was continuously circulated through the column consisting of geotextile material at the base, followed by a 61cm layer of tire shreds and another layer of geotextile and lastly, a 15.24cm thick top layer of silica sand. The stopcock at the effluent end of the column was opened to start the continuous flow test which lasted for one week with the pump flowing

at a rate of 2ml/s. Three samples were collected twice per day and tested for pH, total organic carbon (TOC), turbidity and iron.

The pause flow test was next conducted by closing the stopcock at the effluent end of the column and turning off the peristaltic pump. Rainwater was left in the column and samples of the leachate were collected and tested intermittently by turning the pump on and opening the stopcock. The test column test showed that it is preferable to construct the embankment above the water table because the tire shreds will have no significant effect on the surrounding since the soil will be free draining (based on the continuous flow experiment). Tests on leachate from crumb rubber fills have produced no deleterious impacts to the environments (Pierce and Blackwell 2002). It was shown that scrap tire rubber can absorb and retain volatile organic compounds (VOC's).

In a similar experiment, Humphrey and Katz (2000) carried out a five year study of the water quality effects of tire shred fills placed above the groundwater table by collecting leachate from beneath a field trial constructed beneath a secondary state highway in North Yarmouth, Maine. The samples were collected in three 3-m square geomembrane lined basins located beneath the shoulder of the road. The results of the study showed that there was no evidence that the presence of tire shreds altered the concentrations of substances that have a primary drinking water standard such as barium (Ba), cadmium (Cd), chromium (Cr), lead (Pb), and selenium (Se) from their naturally occurring background levels. In addition, there was no evidence that tire shreds increased the levels of aluminum (Al), zinc (Zn), chloride (Cl-) or sulfate (SO4), which have secondary (aesthetic) drinking water standards. In a few samples, iron (Fe) levels exceeded their secondary standard. Manganese (Mn) levels consistently exceeded their secondary standard, however, this is an esthetic standard. Three sets of samples were tested for organics and the results showed negligible levels of organics.

Subsequently, Humphrey and Katz (2001) also conducted field trial/quality tests on water samples collected from wells bored in and around tire shred filled trenches. However, the trenches were situated below the water table this time around so that they could determine the likelihood of leachate from the tire shreds into the water and the levels thereof. The study consisted of three sites each having 1.4 metric tones of tire shreds buried in a trench below the water table. Maximum sizes of tire shreds were

75mm. Samples were taken over a four year period and analysed for various metals, volatile and semi-volatile organic compounds.

Results of the test showed that the tire shreds had negligible effect on the concentration of metals with primary (health based) drinking water standards while concentrations of iron and manganese exceeded secondary drinking water standards. However, since secondary standards apply to aesthetics and not health, this was a minor concern. Levels of organic compounds in the leachate from tire shreds located below the water table were detectable. Hence, several standards specify that applications involving tire shreds should be confined to locations above the water table until it is confirmed that these detectable levels are no threat to human health.

2.3 Applications of Recycled scrap tires in Construction

Scrap tires have been used in construction as lightweight road embankment fill, backfill behind walls, insulation to frost penetration beneath roads and heat flow to pavement surface, aggregate in leachate (preferably with a neutral pH), aggregate in drainage bed for residential septic systems and gas collection systems in landfills. The tire shred layer in each application is usually separated from the surrounding soil by covering it with geotextile material to prevent infiltration by soil which leads to undesirable results such as settlement.

They are blended for use in pavement binders and sealants or as an aggregate substitute in Civil Engineering systems. An example of such a binder is Rubber Modified Asphalt (RMA) which increases the durability and life of asphalt but costs almost twice as regular asphalt although this area is still under study (Maryland Department of the Environment 2005).

Siddique and Naik (1995) showed that the introduction of discarded tires into asphalt or mortar results in higher skid resistance, reduced fatigue cracking and longer pavement life than normal asphalt. Scrap tire ash (obtained as the residue of tire rubber chips burnt at a controlled temperature of 80° C for 72hrs) can also be used in concrete in the form of tire rubber ash (Tire Rubber Ash). Rubcrete can be used for nailing concrete, constructing false facades and interior construction because of its light unit weight (9 to

16 kN/m^3) as well as in highway construction as shock absorber in sound barriers and earthquake shock-wave absorber in buildings.

Chu (1998) constructed a test embankment made up of 30% shredded tire material and 70% clay soil by weight and monitored the settlement, slope stability and leachate composition for one year. During this period, the slope angles of the test embankment remained constant and the maximum settlement was approximately 15cm. The slope stability analysis indicated that the test embankment had a factor of safety of 4.1 under dry conditions and 2.1 under saturated conditions. The environmental effects of the shredded tire and soil-tire mixtures were evaluated by performing the loss on ignition test (LOI), bulk chemical analyses and leachate analyses.

The LOI test involved heating the dry shredded tire in a furnace at high temperature (approximately 1000°F) into ash form and determining the percentage loss of impurities by taking the ratio of the weight lost to the initial weight of the tires. The bulk chemical analysis test involved burning the shredded tire of a given size range (weighing approximately 1gm) in a muffled furnace, treating the resulting ash chemically, filtering and analyzing the constituent elements by using an Inductively Coupled Plasma Spectrometer (ICP) . The average LOI and bulk chemical analyses of twenty samples of each tire size range and their standard deviations were obtained. The t-test was then applied to assess the effect of tire chip sizes on the mean LOI and bulk chemistry.

Results of the LOI test and bulk chemical analysis test showed that pure tire material could adversely affect the environment if the tire chips were to degrade completely and all components were to be released. The results of leachate tests on shredded tires exposed to the air showed that the clay-tire mixtures used are less likely to contaminate the environment when the proportion of shredded tire material was less than 60%.The results on leachate from the embankment showed that the concentrations of heavy metals were not above recommended limits by Environmental Protection Agency (EPA, 1990) and that they decreased with increasing depth.

Chung and Hong (2002) developed a new pavement material called elastic and permeable pavement material (EPPM) to meet both requirements of permeability and elasticity using waste passenger tires as the scrap rubber source.

Shredded rubber tires can be used as lightweight backfill material for embankment construction either alone or mixed with soil. Youwai and Bergado (2003) developed a hypoplastic model to simulate the stress- strain (or strength and deformation) characteristics of the shredded rubber tire and sand mixtures (at various ratios) for use as lightweight backfill material for embankment construction. This model interprets (to a very accurate degree) the positive and negative dilatancy characteristics of rubber and sand mixtures previously overlooked by other research works that used a hyperbolic model.

Youwai and Bergado (2004) further explain the state dependent constitutive hypoplastic model by successfully implementing it into a numerical analysis program. Three stages were involved, first the constitutive model of fill material for rubber tire chips and sand mixtures was converted into finite difference program. The results of triaxial test were then compared with the corresponding results from the numerical analysis. Next, the reinforced wall using rubber tire chip-sand mixtures as fill material on rigid foundation was simulated. Lastly, the parametric study on the effects of reinforcement stiffness and interface shear stiffness on the behavior of the reinforced wall was carried out. This was then used to simulate the behavior of the reinforced wall on rigid and soft ground.

Cecich et aL (1996) tested the viability of using shredded tires as lightweight backfill material for a retaining wall system required to provide an adequate level surface for a proposed roadway. The soil at the project site was predominantly silty clay, which was excavated and replaced with the shredded tires. This is because silty clay possesses very poor drainage characteristics which results in the build-up of hydrostatic pressure behind the wall which means building a larger retaining wall and incurring increased costs as a result. The cost of the retaining wall designs for three different heights of 3,6 and 9m of 30.5m length using the shredded tires were compared with that using conventional backfill sand. It was determined that using a shredded tire wall instead of sand wall would generate an average saving of 60%. A cantilever wall was selected for the design which consisted of two parts namely the geotechnical design such that the wall satisfies the external stability requirements and the structural design which involves determining the amount and type of concrete and reinforcement needed.

Humphrey (1998) constructed an embankment on soft clay with tire shreds as an alternative to conventional soil which would have been so heavy that it would have sunk into the clay. The Maine Turnpike Authority (MTA) wanted to build the embankment as part of an interchange to provide better access to the Portland, Maine Jetport. It was supposed to meet the recommendations by ASTM D 6270 (1998) that ensured that self heating was limited. Two layers of lightweight tire shreds were chosen, each measuring up to 3m thick and separated by a 0.915m clay layer. The sides and top of the embankment were covered by 0.915m tro 1.83m of clay. The size of tire shreds used was about 300mm. The Maine Turnpike Authority (MTA) was able to save $300,000 over the cost of the next cheapest construction alternative (that is, expanded polystyrene insulation board) by using the tire shreds.

Li et al (2004) investigated the use of large sized fibers and NaOH-treated chips in the production of pavement concrete since it is expected that it will cost much less to produce large sized chip or fiber-modified concrete. The toughness of the modified concrete was greatly enhanced because the rubberized concrete absorbed more energy during the splitting tensile test than normal concrete. This property allows rubberized concrete to resist crack propagation and absorb dynamic loading.

Shalaby and Khan (2005) studied the effects of using large sized shredded tires as lightweight fill for constructing durable geotechnical and cost effective embankment structures. The low unit weight of the tire shreds and their non-biodegradable nature were some of the properties considered before deciding on using scrap tires.

Edil et al (2004) studied the use of scrap tires to eliminate volatile organic compounds (VOC) from contaminated water or leachate emanating from landfills thus alleviating the problem arising from diffusive transport (contaminant migration driven by the difference in concentration between the upper and lower sides of a landfill liner).

Styrene butadiene rubber (SBR), a non polar material, is one of the major components of rubber which attracts non polar organic compounds such as benzene, toluene and trichloroethylene. This further explains why tire chips have a high sorptive quality and that only 3.5 to 7.9% of the absorbed organic compounds are desorbed. Now it is possible to determine the thickness of the tire chip layer and the mass of tire chips needed to remove a given amount of organic compounds through equations. Tire chip

layer thickness ranging between 0.3 and 0.45 is recommended for general landfill applications.

However, the tire chip size does not play a significant role in determining the rate of sorption of organic compounds which rather is a function of the diffusion coefficient. Tire chip sizes between 0.05 and 0.3m are recommended for use as substitute for landfill leachate collection media. The effectiveness of shredded scrap tires in retarding transport of organic contaminants in a solid waste landfill studied through large-scale laboratory tests.

Garga and O'Shaughnessy (2000) identified earth fills that were successfully constructed using whole scrap tires in several countries including the United States of America, England, France, Germany, Brazil and Switzerland and appraised their level of performance. One of the first reported applications using scrap tires was the repair of a hillside fill instability along California Highway, north of Santa Cruz in the mid-1970's.The road embankment was rebuilt by reinforcing the soil with tire sidewall mats that were vertically spaced at 0.6m and joined together by steel clips to form a continuous mat that was extended beyond the embankment face by 100 - 150mm to prevent erosion. The tire sidewall mats facilitated the construction of a side slope of 2 to 1 rather than the typical 2 to 3 which resulted in savings of about 70,000m^3 of costly fill.

In England, scrap tires were used in constructing an experimental gravity wall in West Yorkshire (1977) so as to provide extra space for future office expansion or car parking. Whole tires (ranging between R-13 to R-15 inch radius) from cars or light commercial vehicles were used having widths ranging between 125 and 200mm. The height of the tire wall varied up to 3.7m and incorporated a curve. The length of the structure (made up of 4,500 tires) was 45m with an average tire layer thickness of 0.15m creating a useable area of approximately 100mm^2.This approach saved about three quarters of the amount that would have been spent constructing a conventional retaining wall.

Other applications of tire reinforced soils include energy absorption barriers for rockslides and snow avalanches, arching to reduce load distribution above buried culverts and improving ground serviceability for military vehicles. Structurally, it can be used for creating artificial islands and reef, land terracing crash barriers, bridge abutments sea

defenses, stabilizing soil heaps, soil foundations to mention a few. A test fill was constructed at an automobile recycling yard near Ottawa and used as the case study for investigating the behavior of tire- reinforced structures. In all, approximately 10,000 whole and cut tires were used.

Flowable fill is a self-leveling and self-compacting material that is now widely used in construction and crumb rubber is its main constituent. The flowable fill produces a mass density ranging between 1.8 and 2.3 g/cm^3 when mixed with concrete sand. Pierce and Blackwell (2002) replaced sand with crumb rubber to give a lightweight material that could be used in construction applications such as bridge abutment fills, trench fills and foundation support fills.

The other components of a typical flowable fill material are cement, fly ash, fine aggregate (concrete sand) and water. However, to perform effectively, flowable fill must meet flowability and bleeding requirements in its fluid state. Hence, the crumb rubber must be optimized to satisfy both requirements. Other factors such as mixing speed, mixing time and fly ash content can be increased to control the bleeding.

Due to its low specific gravity, crumb rubber can be added to flowable fill to produce a lightweight material. The bulk density decreases as the crumb rubber content increases producing densities between 60 to 80 % that of standard flowable fills mixed with sand. The result is a material that can be used for lightweight construction on soft and compressible soils and which imparts less stress on the soil beneath it thereby reducing soil settlement.

In order to verify the effectiveness of recycled scrap tires as lightweight backfill material for retaining walls, Humphrey and Tweedie (2002) studied the performance of a retaining wall test facility with tire shred as backfill material instead of gravel. The results were then compared with that of the North Abutment of the Merrymeeting Bridge also with tire shred backfill. The abutment was constructed as part of the Route 196 Bypass project in Topsham, Maine and the main reason for using tire shred backfill was to improve its factor of safety against rotational slope instability. The tire shreds used were obtained from three sources and varied in size from 38mm to 76mm while the maximum average field density was 0.71Mg/m^3.Horizontal stresses under surcharges up to 35.9 kPa in both cases were measured with pressure cells. The results showed that

under at rest conditions with surcharge loads less than 12.0kpa, the horizontal stress increases with depth whereas as the surcharge increases, the horizontal stress nearly becomes constant with depth.

Also, the at rest horizontal stress measured for tire shreds is 45% less than that of typical granular fill and the horizontal stress for the tire shreds decreases as outward rotation of the wall increases. They observed that the coefficient of lateral earth pressure at rest, K_o decreases with depth at each surcharge. Also, that K_o increases as the surcharge increases up to 23.9kPa and remains constant from 23.9 to 35.9kPa. In conclusion, they discovered that the coefficient of lateral earth pressure, K was independent of tire shred size.

Humphrey et al (2002) studied the use of scrap tires (tire chips) as insulation material to reduce the depth of frost penetration beneath roads. A field trial was constructed in Richmond, Maine on a dead –end gravel road with control sections and test sections containing tire chip layers varying between 152mm and 305mm in thickness. Subsurface temperatures were measured by using thermocouples.

It was observed that the tire chip layers reduced the depth of frost penetration by between 6 to 20 percent compared to a control section, the higher percentage reductions corresponding to colder than average winters. Comparison of the control section and the tire chip sections showed that while the freezing front continued to penetrate the deeper into the subgrade soils during the entire winter season, it was only able to penetrate to the bottom of the test sections in the early winter period. There was negligible penetration into the underlying subgrade soil during the remaining winter season confirming the effectiveness of scrap tires as thermal insulators. The thermal conductivity of tire chips were then obtained by using the assumption of a steady state heat flow and continuity relationship between the tire chip layer and the underlying soil based on the subsurface temperature measurements. The thermal conductivity obtained through this process ranged between 0.29 and 0.42 W/m°C.

Shalaby and Khan (2005) studied the performance of a full-scale tire shred test road embankment constructed on soft organic clay in Manitoba. It is instrumented with strings of equally spaced thermocouples to record the thermal behavior of the tire shreds. The adjacent ground was also instrumented with thermocouples to act as control. The

data collected from the measurements showed that the depth of frost penetration ranged from 600mm to 1250mm inside the tire shred embankment and from 300mm to 750mm. This contradicted earlier results by other similar researches. The reason was likely due to the high void ratio of the tire shred embankment (since earlier experiments had used smaller sized tire shreds), the presence of a thicker blanket of snow on top of the natural ground compared to the tire shred embankment and lower water content in the tire shred embankment. In addition, it was established that the thermal profile of tire shreds generally follows the thermal profile of natural ground.

Beyond the use of small sized recycled scrap tires, Yang et al (2001) have also shown that scrap tires (that is, truck tires) can be used whole in the construction of culverts. The structural performance of the truck tires were determined by evaluating the strength and stiffness properties of the truck tire culverts as well as their interaction with surrounding backfill soils. In order to achieve this, parallel plate and field tests were carried out on the culverts, also a culvert analysis and design program that developed structural performance-based design guidelines was used. The recommended range of inside diameter of the truck tire should be between 0.53 and 0.60m while the range of outside diameter should be between 0.99 and 1.07m.

2.4 Challenges to the Use of Recycled Scrap Tires due to its undesirable properties

A major challenge to the use of scrap tires in construction is their susceptibility to fire hazards. The reported ignition and sometimes explosion of tire in fills has been a source of concern. This has been adduced to the exothermic reactions that occur within them. According to Baker et al (2003), the exact mechanism(s) involved in the initiation of exothermic reactions in scrap tire fills remains unknown. Studies of various cases of such incidences show that the exothermic reactions developed as a result of the following mechanisms: oxidation of exposed steel wires, microbes generating acidic conditions, oxidation of rubber and microbes consuming exposed steel belts. The oxidation of iron results in a lot of heat and maybe a major contributing factor to the generation of exothermic reactions and ignition of scrap tire fills. The other mechanisms create suitable conditions for the ignition of a scrap tire fill.

Two examples of such cases in which scrap tire fills have experience exothermic reactions are the Ilwaco project in Washington and the Garfield County Project also in Washington (Baker et al 2003). The Ilwaco project required the use of tire shred fill as lightweight fill to repair a 42.7m gap in a road caused by a landslide. The road was located adjacent to the mouth of the Columbia River. The tire shred layer was 7.93m thick (higher than the 3m height recommended by ASTM D 6270, 1998). The construction of the road commenced on September 23, 1995.The tire shred fill was completely placed in by October 18, 1995 and the road was paved on October 31, 1995.The first evidence of problem was noticed a few days before December 25, 1995 when cracks began to form in the pavement. On January 3, 1996, water vapour and cracks were observed and by late February 1996 the fill had to be removed after realizing that the rate of reaction within the fill was increasing.

The Garfield County project required using tire shred to fill a ravine so as to straighten the gravel surfaced county road. The total height of embankment formed was about 15.1m with about 13.72m of it being tire shreds (comprising about 12,000 tons of shredded tires). The side slopes were 1.5H to 1V.Construction of the fill began in late Fall of 1994 and was completed in Spring, 1995.The tire shreds were originally placed in lifts of 304mm to 457mm and compacted by a bulldozer. The tire shreds placed in the lower part of fill were produced by a hammer mill process which resulted in significant amount of exposure of steel while the shreds in the upper parts of the fill were produced by shearing. Between Spring, 1995 and October 7, 1995, some minor settlement of road crest occurred. Additional pit run gravel was placed in to bring the road back to grade. Fissures and cracks developed in the fill surface and smoke was noticed to be issuing from the cracks on October 7, 1995.Additional fill had to be placed into the embankment because further settlement occurred from October 7, 1995 to through to January 17, 1996. On January 17, 1996, open flames were observed on a 1.2 square meter area of the fill and subsequently had to be removed and disposed at a loss of $2.5 million.

However, there has been no such report concerning recent earth fills constructed in accordance to new design guidelines which minimize internal heating such as ASTM 6270 D (1998). In order to set a tire containing structure on fire, a continuous and intense

application of heat is required and only the exposed tires at the surface are normally burnt.

Another challenge to the use of scrap tires in construction is the possibility of harmful leachate discharges from tire fills into surrounding ground water. Extensive field investigations by Humphrey (2000) and Shalaby (2005) of the leaching effects of scarp tires placed above the ground water table into surrounding water showed that all the metals with primary drinking water characteristics (barium, cadmium, chromium, copper, lead and selenium) were below their regulatory allowable limits (RAL). In the case of the metals with secondary drinking water standards (aluminium, calcium, iron, magnesium, manganese, sodium and zinc) only iron and manganese were detected in levels exceeding their secondary drinking water standard. In terms of organic compounds, negligible concentrations were detected in the water samples. Field study investigations of the effects of scarp tires placed below the ground water table (Humphrey and Katz 2001) show that organic compounds are leached in low concentrations. In addition, the levels of manganese and iron released by the scrap tires in this case exceed their secondary drinking water standards eventhough this is not considered hazardous to health since they only affect aesthetics. This justified the recommendations made in ASTM D 6270 (1998) that all scrap tire fills should be constructed above the ground water table because of the unknown effect of the organic compounds.

2.5 Appraisal of Field Investigation of Embankments Constructed with Recycled Scrap Tires

Zvanut (2003) monitored the settlements of a 9m high embankment located on marshland soft soil in Barje, Slovenia by field instrumentation consisting of ten settlement plates and one measuring tube which was installed beneath the embankment and used to assess the settlement profile of the embankment via a hydrostatic profile gauge. The embankment was constructed in two layers, the lower strata was 3m high and made from ash obtained from a thermo-electric power plant whereas the upper strata made from crushed stone was 6m high. The settlement plates were laid in 3 lines across the embankment at the bottom of the lower stratum of the embankment slightly before the commencement of construction works. The measuring tube was placed in an ash stratum

about 1m below the upper stratum of the crushed stone embankment. Movement of the plates was determined by conventional geometric leveling while the vertical movement of the tube at points 0.5m apart was monitored using a hydrostatic profile gauge. The hydrostatic profile gauge consisted of a control unit, a readout unit and a length of triple tubing connected to a settlement probe which can be pulled or pushed through the access tube. The settlements measured by the hydrostatic profile gauge showed a continuous increase in the vertical displacement after the construction for approximately half a year and the maximum measured settlement was 43cm. The results obtained from the prfile gauge were very similar to those from the one of the settlement plates located 2m below it.

Hoppe and Mullen (2004) studied the field performance of an experimental highway embankment constructed with a mixture of shredded tires and soil. It was instrumented and monitored for several years following construction. The embankment is located at the intersection of Route 199 and Route 646 Connector in York County, Virginia approximately 3km North of Williamsburg. It was one of two embankments constructed North and South of the Route 646 Connector in the year 1993, each containing a shredded tires section adjoining a conventional soil section.

The shredded tire embankment section under study (North Embankment) was 80m long with maximum shredded height of approximately 6m.It was terminated by a soil section approximately 30m long so as to facilitate future bridge construction linking it with the South embankment over the route 646 connector. A 50/50 volumetric ratio of shredded tires to soil was used to build the shredded tire section and the soil was yellow silty sand. The tires shred used conformed to the special provision by the Virginia Department of Transportation (VDOT) for shredded tire fills which requires that the maximum length be 25cm, maximum surface area be 260cm^2 and pieces should not have loose metal strands.

The topography is generally flat with no streams nearby. The depth of ground water table below the original ground surface was 7m. Geologically, the soil consisted of mixtures of sand, silt and clay. Geotechnical borings were drilled in the foundation soil before the embankment was constructed .The subsurface soil underlying the shredded tire

section was more compressible than the soil underlying the conventional embankment section.

Settlement sensors were placed at the top and base of the embankment while earth pressure cells were installed at the base in both the shredded tire/sand sections and the conventional sand sections. All sensors were of the vibrating wire type. A Campbell Scientific Cr-10 Datalogger was used for data collection and storage and a data were retrieved periodically for analysis with a portable computer. Groundwater monitoring of leachate effects from the tire/sand fill mixture was conducted by installing two groundwater wells. One well was placed at the toe of the shredded tire section while the other was located upstream. The wells were sampled quarterly for the first year and then semiannually thereafter.

Elements and parameters monitored included calcium, magnesium, sodium chloride, iron, lead, zinc, hardness, pH, total organic carbon, total organic halides and specific conductivity. Embankment temperature measurements were carried out in 1996 using a portable infrared thermometer as well as a Texas Instruments Nightsight Infrared camera with the aim of detecting potential localized heat sources.

Forty five temperature readings were collected on top of each embankment section in February 1996, the average recorded temperature being 7.2C and 6.9C on top of the soil and shredded-tire embankments respectively. In May 1996, additional temperature monitoring was carried out by taking infrared scans along the embankment. No signs of exothermic reaction were detected in the embankment during the 10 year monitoring period.

The vertical stress developed in the soil section at the end of the construction and after placement of the surcharge was greater than that developed in the tire/soil section. The ratio was about 0.44 between the soil and tire/soil sections. This indicates that the tire/soil fill reduced the load transferred to the foundation soil by half as much as the load from a conventional soil fill of the same dimensions. Laboratory results indicate that the vertical stress exerted by a soil/tire embankment is roughly 0.6 of the stresses exerted by a conventional soil embankment of the same geometry.

In December 1993, that is 4 months after construction, settlement measurements showed that the tops of the embankments had settled 52 and 30mm in the shredded-tire and soil sections respectively. This indicated a high void ratio in the tire/soil section.

Groundwater monitoring results showed that the use of shredded tires in highway embankments does not create an adverse environmental impact on groundwater quality. This is based on the fact that the measured levels of calcium, magnesium, sodium, total organic halides, total organic carbon, specific conductance, chloride and other elements/parameters in the groundwater samples tested did not show any change from that of control water samples.

The use of large tire shreds mixed with sandy soil does not result in an exothermic reaction within an approximately 6m high embankment, vertical soil pressures exerted by shredded-tire embankments (50/50 volumetric ratio of tires to soil) on the foundation soil are approximately one half of the corresponding stresses exerted by conventional embankments. Shredded tire embankments may also be expected to settle at about twice the magnitude of conventional embankments.

2.6 The Influence Diagram

The influence diagram consists of directed acyclic graphs with nodes and arcs. There are three types of nodes namely chance, decision and value nodes and are drawn respectively as circles, squares and a rounded rectangle. The nodes by nature could be deterministic (meaning that there is certainty about its value) or probabilistic (meaning that there is uncertainty about its conditioning variables).There are two types of arcs namely conditional arcs (which update the chance and value nodes) and informational arcs (which update the decision nodes).

The influence diagram obeys a number of laws paramount of which is that there must not be any directed cyclic paths. There should also be asymmetry in the definition of the arcs such that a conditional arc into a chance or value node indicates that there may be dependence while an informational arc into a decision node indicates that the information must be available at the time of making the decision. The conditional arcs do not indicate causality or time precedence as exhibited by the informational arcs.

Flowcharts are used to indicate the sequence of activities and events in a decision analysis system whereas influence diagrams are organized displays of decisions, uncertain events and outcomes which provide a quick view of the system being represented at any point in time. They resemble decision trees because they are also descriptive tools but the difference between them, according to Pfeiffer (1997) is that the relationships between the various elements of a decision problem are easier to display using influence diagrams than using decision trees.

Bayraktarli Y. Y. et al (2005) showed how an influence diagram can be used to manage earthquake risk. Figure 2.3 shows the influence diagram and the variables considered.

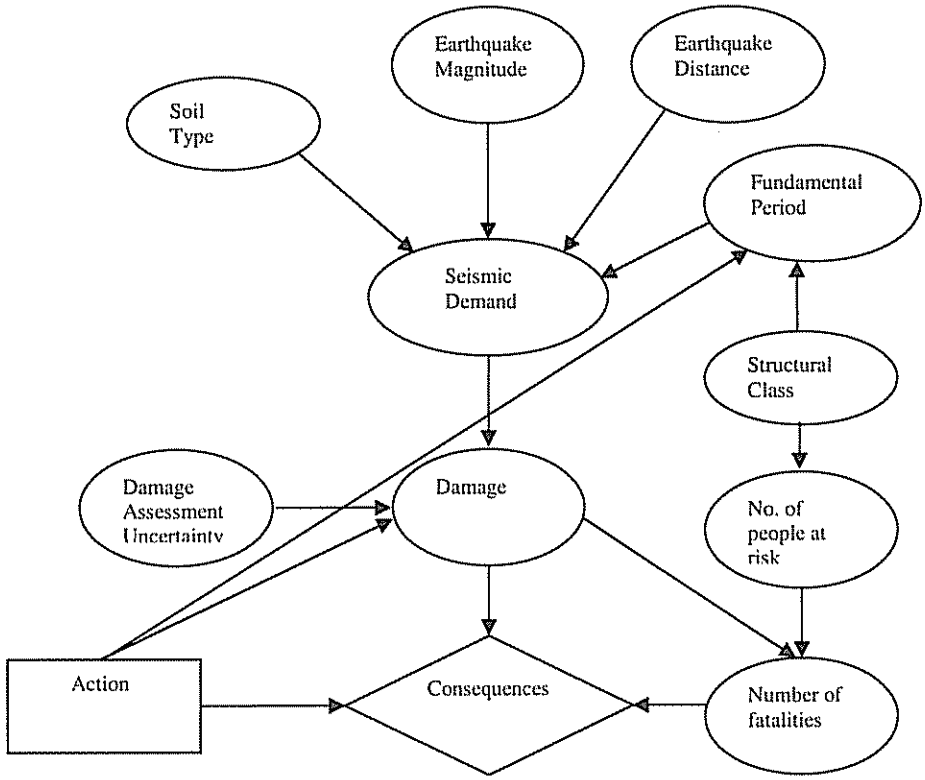

Fig. 2.3 Influence diagram for earthquake activity (Bayraktarli et al 2005)

The influence diagram is used to predict how the soil type, magnitude of earthquake, earthquake distance and fundamental period variables affect the seismic demand. The fundamental period characteristics are decided upon based on structural class, number of people at risk and number of fatalities while the damage characteristics

depend on the damage assessment uncertainty and the seismic demand. The consequences of the earthquake are based on the damage and number of fatalities characteristics. The optimal decision is dependent on the outcome of comparing the expected total consequences of the alternative action. Figure 2.4 shows the equivalent decision tree for the influence diagram in Figure 2.3.

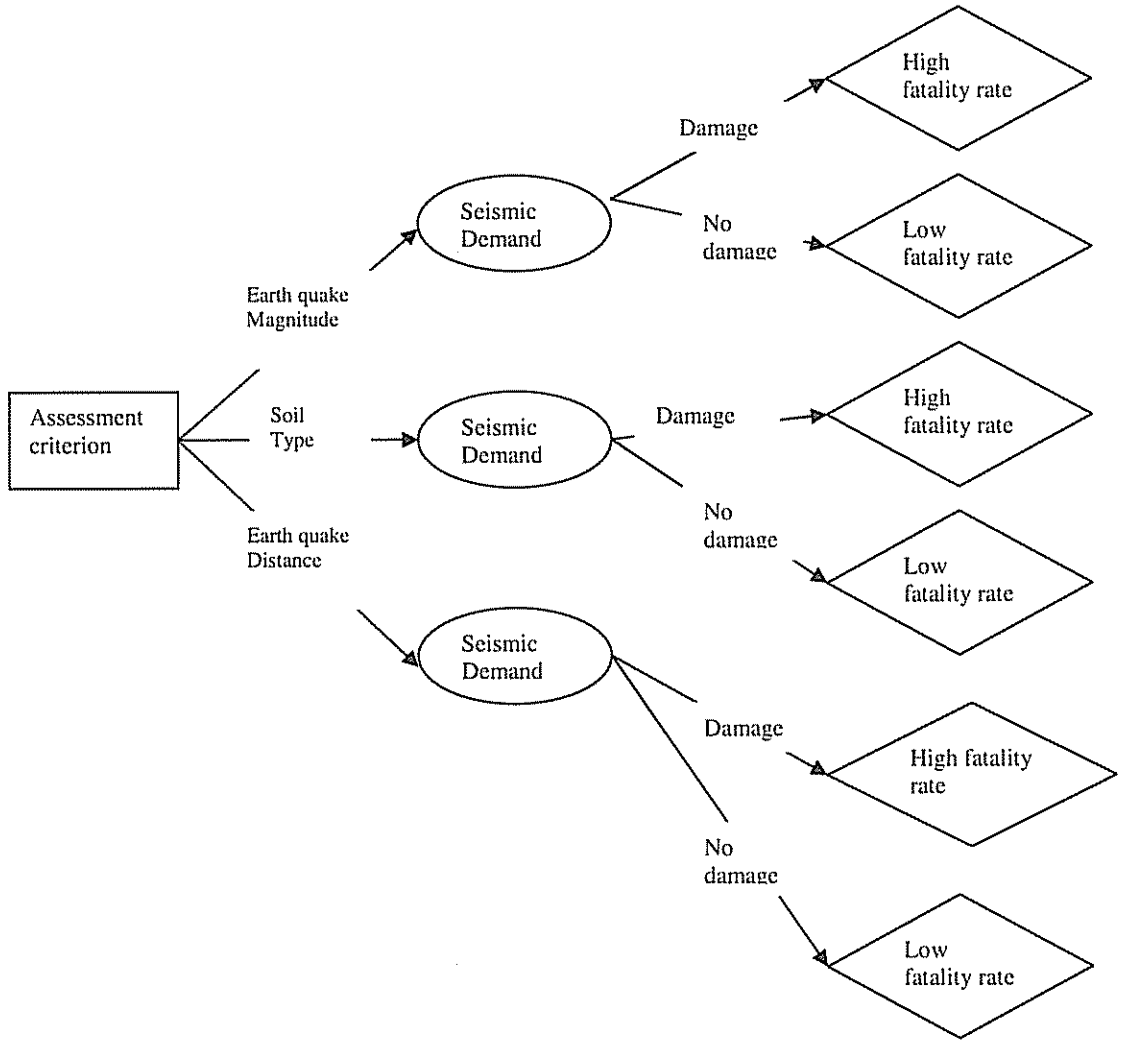

Fig. 2.4 Equivalent decision tree for earthquake activity

Hence, an influence diagram is said to be regular if it satisfies two other conditions other than being acyclic namely that the value node (if present) must have no successors and there is a directed path that consists of all the decision nodes (the 'no

forgetting property'). Table 2.2 shows how the symbols representing each component in a typical influence diagram built using typical decision software.

Table 2.2 Symbols Representing Component parts of an Influence Diagram

Symbols	Description	Explanation
	Chance variable	An uncertain variable not under the direct control of the decision maker
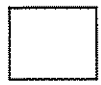	Decision variable	A policy variable under the direct control of the decision maker
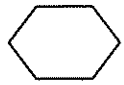	Objective node	Used for quantifying the degree to which decisions satisfy the stakeholders or a measure of utility with multiple goals.
	Index variable	A variable used to define the scope and level of detail of the analysis and identify the dimensions of tables or arrays — such as time
	Standard variable	A variable that is a deterministic function of its inputs
	Module	Nodes that contain a set of variables that comprise a sub diagram of the main diagram.
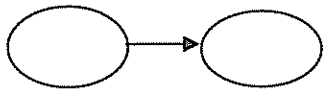	Two chance nodes and an arc	The previous chance node affects the probability of the subsequent chance node
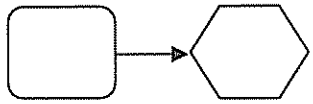	Determinate node, value node and an arc	The occurrence of the outcome depends on the determinate variable
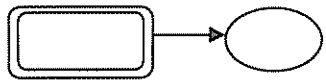	A module and chance node	The chance variable is being conditioned by a variable within the module

2.7 Bayesian Influence Diagrams

Bayesian Influence Diagrams are influence diagrams incorporating Bayesian networks. Bayesian networks are graphical probabilistic models consisting of variables and the cause effect relations between them. A variable may take on values from a collection of mutually exclusive and collective exhaustive states. Bayesian Influence Diagrams maybe discrete having a finite or countable number of states or it may be

continuous, are used for calculating optimal strategies for sequences of actions and incorporate two additional properties of influence diagrams in the network namely decision nodes (rectangles) and utility nodes.

- A decision node allows the user to specify the alternative actions. The parents of decision nodes contain information which is available at the time of making the decision
- Utility nodes have no successors and are preceded by conditional probabilistic and decision nodes. They are measures of the decision maker's preference for each configuration.

The immediate advantage of the Bayesian Influence diagram is that each variable comprising a system may have more values than true and false statements and not all relations have to be deterministic. It could be applied to a wide range of problems including medical diagnosis, mildew control, animal breeding and image analysis.

The Bayesian Influence diagram can then be easily used to develop a model in which the outcome can be compiled as the marginal distribution of all variables in the domain and local dependencies can be modeled as the probabilistic dependence of one variable on the other variables. The method allows for easier deduction of the outcome based on observed evidence than other methods as well as easier updating of the remaining variables in the model.

Some terms used in Bayesian Networks are:

- Child node: a variable which is dependent upon other variables
- Parent nodes: these are nodes directly preceding the child node.
- Root nodes: these are nodes which have no parents
- Leaf nodes: these are nodes which have no children

Bayesian networks are referred to as directed acyclic graphs (DAGs) indicating that loops are not allowed. The Bayesian network gives the joint probability distribution of the entire variable domain, for example let N_v be the number of variables in the domain:

$$U = X_1, X_2, \ldots\ldots\ldots\ldots, X_{Nv}$$

Applying the chain rule to factorization of the joint distribution gives a chain of conditional probability distributions:

$$P(U) = P(X_1, X_2, ... X_{NV})$$

$$= P(X_1 | X_2, ..., X_{NV}) \; P(X_2 | X_3, ..., X_{NV}) ... P(X_{NV})$$

$$= \prod_i P(X_i | pa(X_i))$$

where $P(X_1, X_2, ... X_{NV})$ is the joint distribution of X_1 *to* X_{Nv}

$P(X_1 | X_2, ... X_{NV})$ is the conditional distribution of X_1 given $X_2, ..., X_{Nv}$

$pa(X_i)$ is the set of parent variables of the variable

Inference can then be made of a variable such as X_1 in terms of its parent variables as:

$$P(X_1 | X_2) = \frac{P(X_2 | X_1) P(X_1)}{\sum_{all\ i} P(X_2 | X_1 = x_i) P(X_1 = x_i)}$$

this is a simple model which can be used to analyze large systems under varying situations as long as the network is small and each node represents a few number of states.

For a network with multiple pieces of evidence, a number of efficient algorithms have been developed to ensure that all the nodes are updated with regards to all pieces of evidence. Such algorithms include those that are based on arc reversal and removal and those based on junction trees.

2.7.1 Causal Networks

Bayesian influence diagram are simply causal networks in which the events are represented by nodes and their interdependencies are represented by arcs. Figure 2.5 shows an aspect of the model developed to simulate the embankment response.

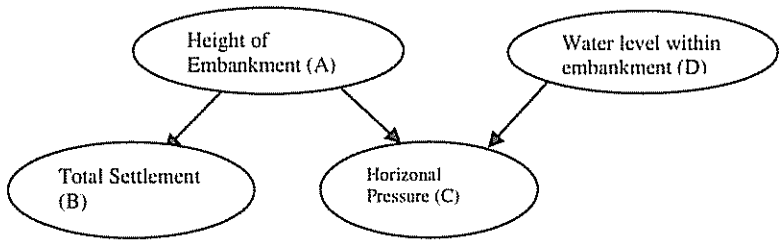

Fig 2.5 Causal Network

Figure 2.5 is an example of a causal network. A causal network consists of a set of variables and a set of directed links between variables. Mathematically the structure is called a directed acyclic graph because it does not consist of cycles. The link from A (height of embankment) to B (total settlement) indicates that B is a child of A, and A is a parent of B.

The variables represent events and in Figure 2.5, each variable has two states (high and low or Yes and no) reflecting whether a certain event had taken place or not and to what magnitude. Generally, a variable can have any number of states, for example a variable can be the cost of an item, type of disaster etc. Variables may have a countable or a continuous state-set but in this work the variables are considered to have a finite number of states.

A variable C (horizontal pressure) as shown in Figure 2.5 has dual causes, A and D meaning that either variables A or D or both have effect on the magnitude of horizontal pressure developed in the embankment. The cause and effect relationships between variables are based on a conditional relationship expressed by the Bayes theorem.

2.7.2 Conditional probability and the Bayes theorem

The underlying principle in the Bayesian treatment of certainties in causal networks is the conditional probability. A conditional probability statement is normally stated in the form: "Given the event a (and all other conditions on b are irrelevant), then the probability of the event b is x"

The mathematical form of this statement is given as:

Probability of $x = P(b|a)$

$$= P(b, a)/P(a)$$

where P(b, a) is the probability of the joint event $b \Lambda a$.

A very important relationship from equation ( ) which can be used to analyse the conditional relationship between the variables is as follows:

$$P(b|a)P(a) = P(a|b)P(b)$$

This gives the Bayes theorem as:

$$P(b|a) = P(a|b)P(b)/ P(a)$$

This equation is used to solve for the probabilities in each variable contained in the Bayesian influence diagram.

Hence, the major properties of a Bayesian Influence diagram according to Jensen (2001) are:

- a set of variables and a set of directed edges or arcs between variables.
- each variable has a finite set of mutually exclusive states.
- the variables together with the directed edges form a directed acyclic graph (DAG).
- to each variable B with parents A_1 ..... A_2 is attached a conditional probability table $P(B|A_1 . . . . A_n)$.
- if B has no parents then the table reduces to unconditional probabilities P(A).
- value nodes which give the utility cannot have children

2.8 Algorithms for effective evaluation of influence diagrams

There are two types of algorithms namely:

1) Value preserving reductions of the initial influence diagram by successive elimination of the nodes:

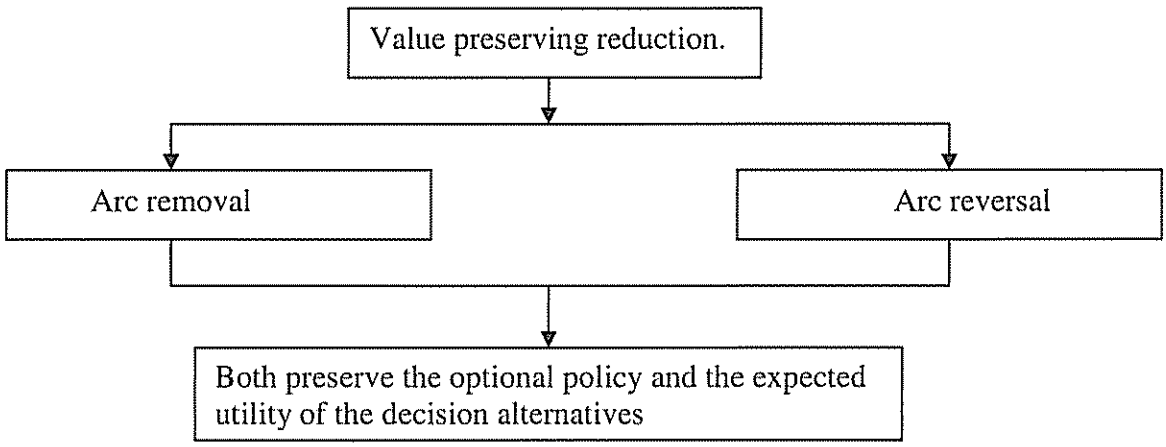

Fig. 2.6 Value preserving reduction method for analyzing influence diagrams

2) Transformation of influence diagram into a junction tree with special properties (Jensen 2001).The junction tree has the following properties:

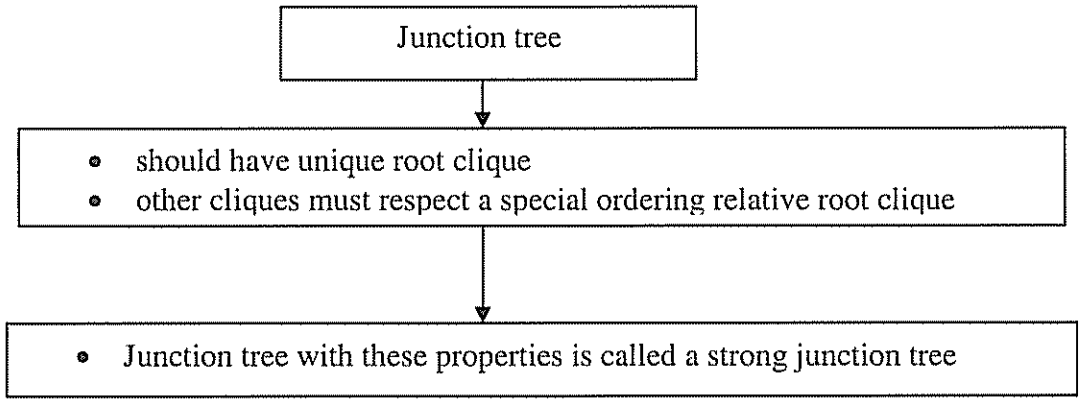

Fig. 2.7 Junction tree method for analyzing influence diagrams

be altered as more knowledge becomes available. Hence, an influence diagram serves as a dynamic decision model for obtaining the optimal strategy. The effects of different scenarios can be investigated by replicating the situations with insertion of evidence.

2.8.1 The Concept of Arc Reversal

Arc reversal, according to Kjærulff et al (2005), is the process used for making inference in probabilistic networks. A typical example of an arc reversal scheme is illustrated in Figure 2.8. where the information travel undergoes a reversal of direction:

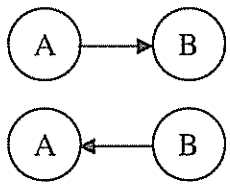

which is expressed mathematically as $P(A,B) = P(B \mid A)P(A)$

which is expressed mathematically as $P(A,B) = P(A \mid B)P(B)$

Fig. 2.8 An arc reversal scheme

Illustration:

In a situation where the posterior marginal distribution for X given evidence on Z is required. Using Shacter's arc reversal procedure, the solution is obtained as follows:

$$
\begin{aligned}
P(X|\varepsilon) &= \eta(\sum_Y \sum_Z P(X)P(Y|X)P(Z|Y)\varepsilon_Z) \\
&= \eta(\sum_Y \sum_Z P(X)P(Y,Z|X)\varepsilon_Z \\
&= \eta(\sum_Y \sum_Z P(X)\frac{P(Y,Z|X)}{\sum_Y P(Y,Z|X)}\sum_Y P(Y,Z|X)\varepsilon_Z) \\
&= \eta(\sum_Y \sum_Z P(X)P(Y|X,Z)P(Z|X)\varepsilon_Z \\
&= \eta(\sum_Z P(X)P(Z|X)\varepsilon_Z \sum_Y P(Y|X,Z)) \\
&= \eta(\sum_Z P(X)P(Z|X)\varepsilon_Z \\
&= \eta(\sum_Z \frac{P(X)P(Z|X)}{\sum_X P(X)P(Z|X)}\sum_X P(X)P(Z|X)\varepsilon_Z) \\
&= \eta(\sum_Z P(X|Z)P(Z)\varepsilon_Z
\end{aligned}
$$

the steps involved and illustrated in figure 2.9 are:

- combine P(Y | X) and P(Z | Y) into P(Y,Z | X);
- Use Bayes' rule to reverse Y → Z which induces a new link X→ Z;
- Using the distributive law, eliminate the barren variable Y ;
- Lastly, use Bayes' rule to reverse X→Z.

Note that if ε_Z represents hard evidence (i.e. Z = z), then the last equation reduces to

$$P(X|\varepsilon) = P(X|Z = z)$$

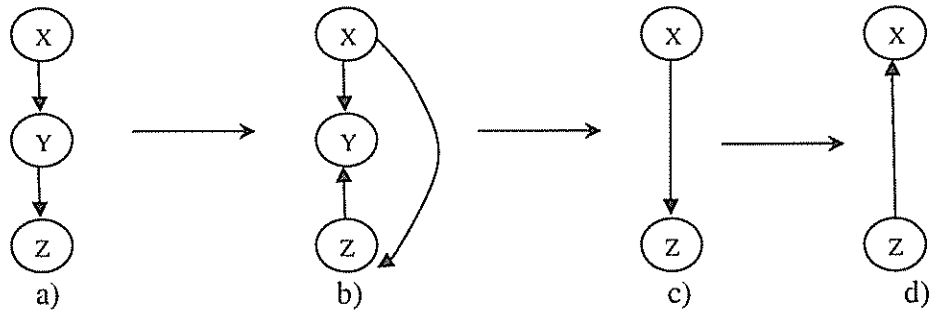

Figure 2.9 Illustration of the Arc Reversal Scheme based on evidence

a) Model for P(X, Y, Z) b) Equivalent model obtained by reversing Y→Z

c) Equivalent model provided that Y is barren d) Equivalent model obtained by reversing X→Z

2.8.2 The Junction Tree Algorithm

Bayesian networks or influence diagrams have been applied to many problem frameworks with uncertainty, such as planning, debt detection, bottleneck detection and diagnosis. However, the major area of application is in the area of diagnosis which is very synonymous to Bayesian Networks. Presently, the most efficient method of updating belief in Bayesian Networks is through the use of junction trees. The smallest clusters of the variables are obtained to form a tree and an information passing procedure is applied to update the beliefs of all the unobserved variables based on the observed variables.

According to Friis-Hansen (2000), a junction tree is a representation of the probabilistic model analogous to that of the network as well as a graphical structure that allows for effective model updating. The nodes are called cliques because each consists of a set of variables from the original network. The junction tree obeys the property that all cliques between two cliques X and Y must contain the intersecting set of variables X ∩ Y called a separator S. A junction tree is constructed by using three procedures namely moralization, deletion and triangulation.

Moralization involves connecting all variables having common child variables by an arc, deletion involves removing the arrows on all arcs and triangulation involves removal of all variables whose neighboring variables are mutually connected and replacing them by their cliques.

In order for a junction tree to be effective, it should have small clique tables and few cliques, the overall goal being to minimize the total sum of the clique table sizes. The size of each clique table depends on both the number of variables in the clique and the number of states in the included variables. Any clique X with N variables has a table t_X of size $|t_X| = N_{I1} N_{I2} N_{I3} N_{I4} \ldots\ldots\ldots\ldots N_{IN}$. Figure 2.10 shows a typical influence diagram.

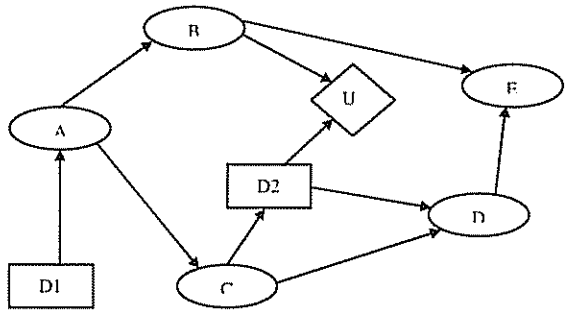

Figure 2.10 A typical influence diagram (Friis-Hansen, 2000).

i) For the influence diagram as shown in figure 2.10 there is a directed path between decision nodes D1 and D2 i.e. $D1 \rightarrow A \rightarrow C \rightarrow D2$

ii)a. Partition the network into sets according to the temporal order of the decisions and the observation of the variables.

b. Set $I_2 = \{D, E\}$: Set of variables observed after the last decision or not observed at all hence eliminate these variables before D2

c. Set $I_1 = \{A, B, C\}$

d $I_0 = \varnothing$: No variables are observed before the first decision

iii). Delete the arcs into the decision nodes and moralize the graph to give figure 2.11:

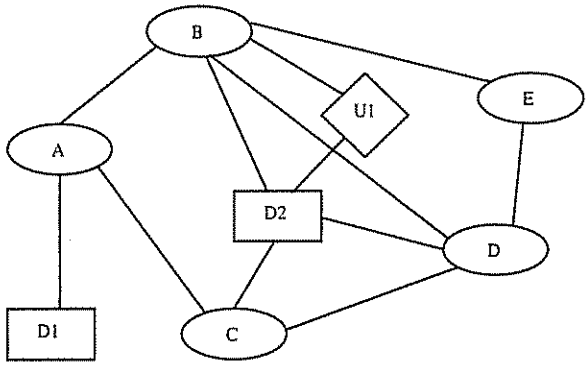

Fig. 2.11 Moralized graph

iv). Remove the utility node, initiate triangulation of influence diagram by removing the variables of set I_2 (figure 2.12) and variable E is eliminated and the clique $\{B, D, E\}$ is formed.

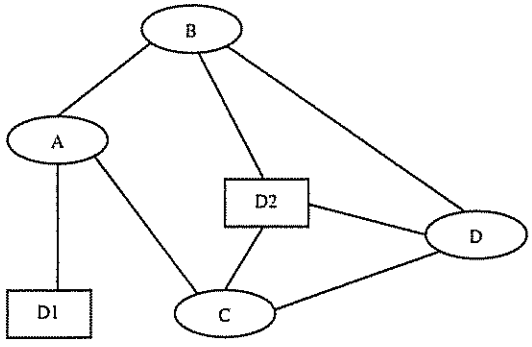

Fig. 2.12 Initiate triangulation of graph

v) Eliminate variable D:

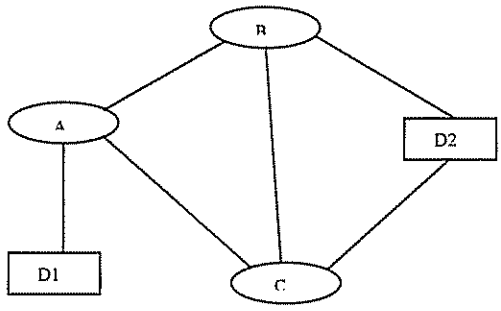

Fig. 2.13 Elimination of variable nodes

Fill-in the link B-C to give the clique $\{B, C, D, D2\}$

vi). Eliminate variable B:

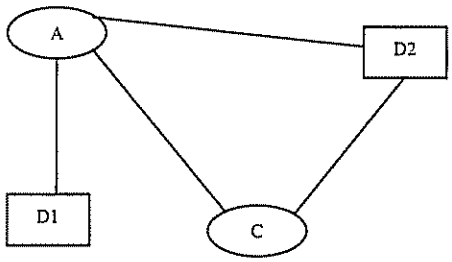

Fig. 2.14 Further elimination of variable nodes

Fill-in link A-D2 to give clique $\{A, B, C, D2\}$

vii). The variables of set I_2 must be removed totally before the variables of other sets. So remove variable A:

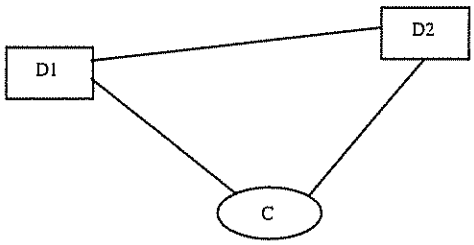

Fig. 2.15 Further elimination of variable nodes

Fill-in links D1-C and D1-D2 to give $\{A, C, D1, D2\}$ .This clique includes all the remaining variables so that subsequent cliques would be subsets of it, no further cliques are formed.

viii). To get the total elimination sequence so as to identify the way the junction tree is connected, the elimination sequence must be completed so that all variables have a number in the sequence. So, eliminate D2 and subsequently eliminate C but no cliques are formed.

ix). Connect the junction tree by identifying the root node using the numbering technique in table 2.3:

Table 2.3 Table showing numbering of cliques

Variable	Variable Number	Clique	Clique Number
E	7	{B,D,E}	7
D	6	{B,C,D,D2}	6
B	5	{A,B,C,D2}	5
A	4	{A,C,D1,D2}	1
D2	3	-	-
C	2	-	-
D1	1	-	-

x). Triangulate the graph;

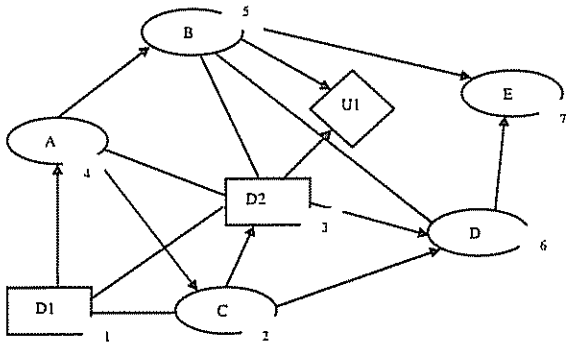

Fig. 2.16 Fully triangulated graph

xi). Form the junction tree:

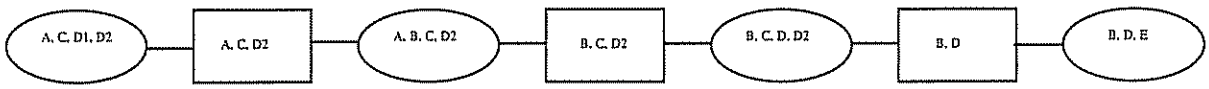

Fig. 2.17 Junction tree

Connect the cliques starting from the root and computing S_k for k>1

$S_5 = C_5 \bigcap \{C_1, C_2, C_3, C_4\}$ using the formular $\Rightarrow S_k = C_k \bigcap \bigcup_{i=1}^{k-1} C_i$

$= \{A, B, C, D2\} \bigcap \{A, C, D1, D2\}$

$= \{A, C, D2\ \}$

and noting that the only clique which contains these variables is clique 1, so connect clique 5 to clique 1 to give;

$S_6 = C_6 \bigcap \{C_1, C_2, C_3, C_4, C_5\ \}$

$= \{B, C, D, D2\ \} \bigcap (\{A, C, D1, D2\ \}, \{A, B, C, D2\ \})$

$= \{B, C, D2\ \}$ - connect clique C_6 to clique C_5

$S_7 = \bigcap \{B, D\ \}$- connect clique C_7 to C_6 to give a strong junction tree (Figure 2.13) .

The tree obeys the criterion that $C_i \backslash C_j$, i>j is eliminated before $C_i \cap C_j$ because $C_7 \backslash C_6 = \{E\}$is eliminated before the set $C_7 \cap C_6 = \{B,D\}$. The variable E is thus only in the leaf clique and does not occur in the cliques closer to the root. Similarly, $C_6 \backslash C_5 = \{D\}$ is eliminated before $C_6 \cap C_5 = \{B,C,D2\}$. Clique 6 is therefore the occurrence of variable D closest to the root. This ensures that information on E and D only occurs in the outermost part of the junction tree.

Further example illustrating the formation of a junction tree from a Bayesian network is shown in figure 2.18 :

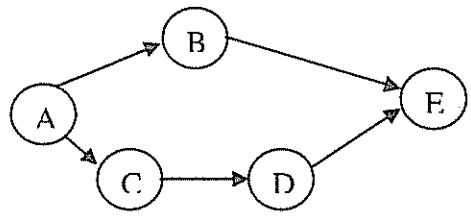

Fig. 2.18 Bayesian network

i) Moralize the graph

a) Remove the direction arrows

b) Connect all the parents of every node with edges

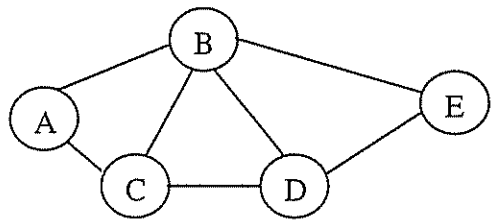

Fig. 2.19 Moralized graph

ii) Triangulate the graph

Add edges to the graph until all the nodes from any cycle are completely connected

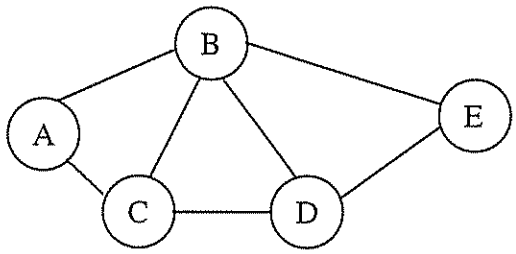

Fig. 2.20 Triangulated graph

iii) Identify cliques:

The clusters form the cliques; ABC, BDC and BDE. Table 2.4 shows the clusters and edges formed:

Table 2.4 Table of clusters and edges

Nodes removed	Cluster formed	Edges introduced
C	ABC	none
D	BDC	BC
E	BDE	BD

The junction tree formed by the process is shown in figure 2.21.

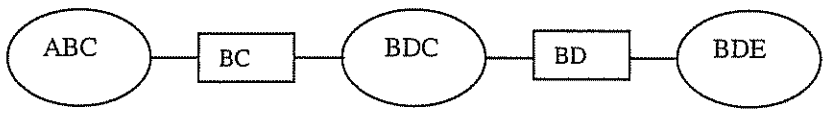

Fig. 2.21 Junction tree

iv) Transfer the potentials:

Define a potential $\Psi_A(X_A)$ in relation to each clique which is a non-negative function on the realization of clique X_A. The potentials of cliques in the hypergraph are initialized using the underlying hypergraph while the potential of the separators are initialized to one.

v) Propagate the information

This is the mode by which information is passed from one clique say A to another say B with potentials Ψ_A and Ψ_B through the connecting separator C which has a potential ϕ_C initialized to unity.

The update equations are as follows:

$$\phi^*_C = \sum_{B\setminus C} \Psi_B$$

$$\Psi^*_B = \frac{\phi^*_C}{\phi_C} \Psi_B$$

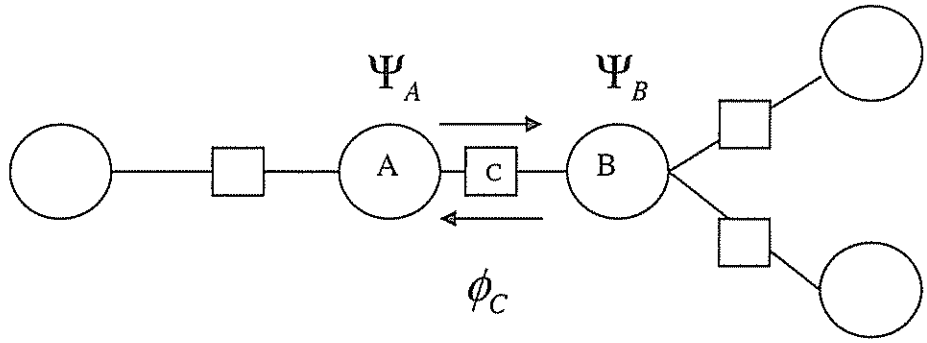

Fig. 2.22 Message propagation in a junction tree (Jensen F. V., 1995)

Once the algorithm terminates, the clique and separator potentials must be proportional to the marginal probabilities and they must be consistent:

$$\sum_{A\setminus C} \Psi_A = \sum_{B\setminus C} \Psi_B$$

The underlying steps therefore are:

a) Partitioning of the network into N_D+1 sets: I_0, I_1 _ _ _ _ I_{ND} according to the decision and the observation order

I_{ND} – set of variables observed after the last decision or not observed at all

I_0 – set of variables observed before the first decision

b) Dropping direction signs on arcs and deleting arcs pointing into decision nodes and utility nodes

c) Moralizing or connecting all parent nodes with common children

d) Triangulation which involves eliminating the variables from set I_{ND} i.e. the N_Dth decision, then I_{ND-1} and so on noting that;

- a clique is formed from the eliminated variable and its neighbors
- a new clique is not formed if all its variables already belong to an existing clique
- the elimination sequence constitutes a numbering of the variables so that the first eliminated variable is assigned the highest number

e) Numbering the cliques

2.8.3 Assignment of probability tables to the junction tree

In order to initialize the junction tree, the first step taken is to assign probability tables to the cliques and the separators by filling them with ones. This is followed by choosing one clique containing the set $\{pa(X_i)\} \cup \{X_i\}$ and the probability table $P(X_i|pa(X_i))$ is multiplied unto it to give the equivalent Bayesian Network model.

The joint probability table is then given as :

$$P(U) = \frac{\prod clique\ tables}{\prod separator\ tables}$$

This table can be used to update the model by inserting evidence as observed in the form of a finding. A finding is defined as a vector f of ones and zeroes corresponding to the possible and impossible states of a variable respectively and it is inserted in a joint probability distribution by multiplying it on $P(U)$.

$$P(U,\mathrm{f}) = P(U).\mathrm{f}$$

The marginal distributions of each individual variable may be found by summation over all other variables known as sum marginalization:

$$P(X_i) = \sum_{U\setminus\{X_i\}} P(U)$$

The order in which the variables are marginalized out does not change the outcome, and the introduction of a finding, f gives:

$$P(X_i|\mathrm{f}) = \frac{P(X_i,\mathrm{f})}{P(\mathrm{f})} = \frac{\sum_{U\setminus\{Xi\}} P(U,\mathrm{f})}{\sum_U P(U,\mathrm{f})}$$

from which any variable such as X_i can be marginalized out.

Hence, two adjacent cliques say X and Y have the probability tables t_X and t_Y and their separator table is obtained by sum marginalization of the separator set S = X and Y so that the separator table $t_s = P(S)$ contains the common information about X and Y:

$$t_s = \sum_{X \setminus S} t_X = \sum_{Y \setminus S} t_Y$$

Message passing between variables can be carried out through the following theories:

a) Hugin propagation theory

Involves message or information passing via two step scheme namely collect evidence step and distribute evidence step. The procedure for executing either step is as shown in figure 2.23.

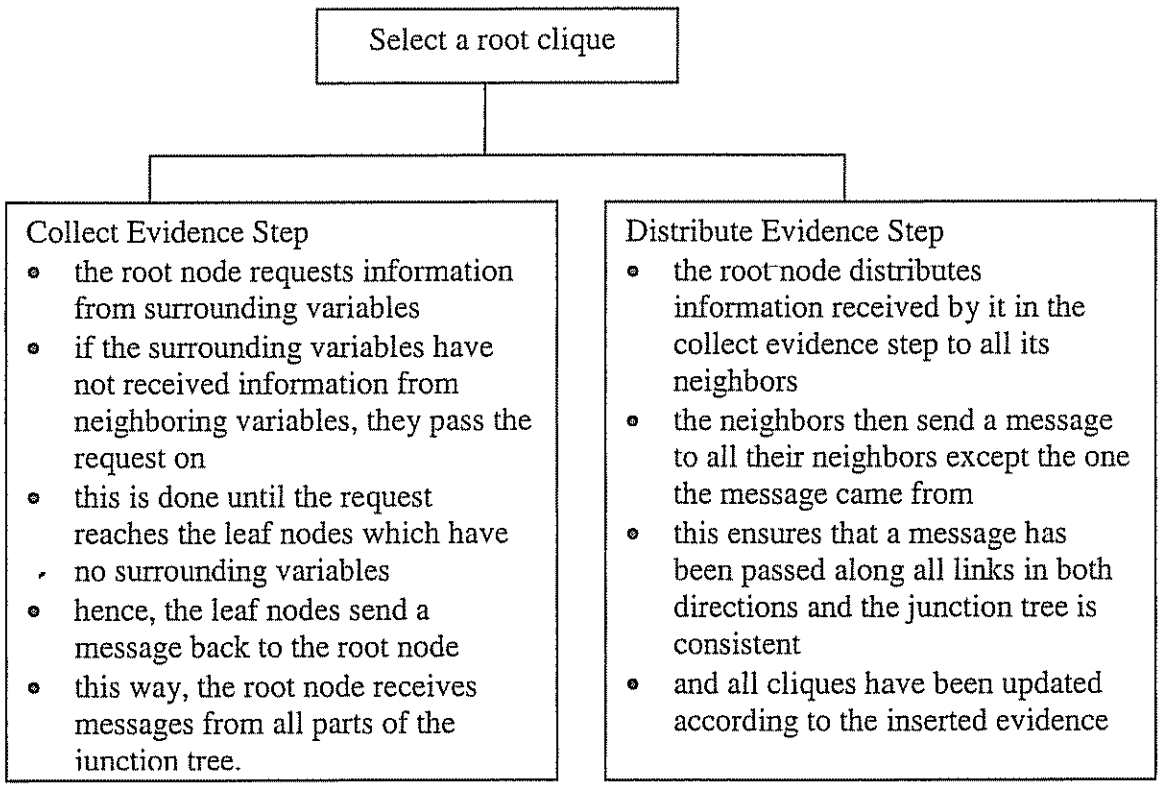

Fig. 2.23 Procedure for executing Hugin propagation (Madsen and Jensen, 1999/ Friis-Hansen, 2000)

b) Max-propagation theory

This involves identifying the most likely configuration (which best explains the observed evidence) of the rest of the variables in the network given evidence on one or more of the variables. A configuration is a set consisting of exactly one state from each

variable. Max-messages are computed by replacing summation with maximization (or max-marginalization):

$$t_s = \max_{X \setminus S} t_X$$

So instead of summing along every dimension in the set X\S, the maximum value is taken and the outcome is information consisting of the maximum probabilities along each dimension. The procedure for finding the most probable configuration is as shown in figure 2.24.

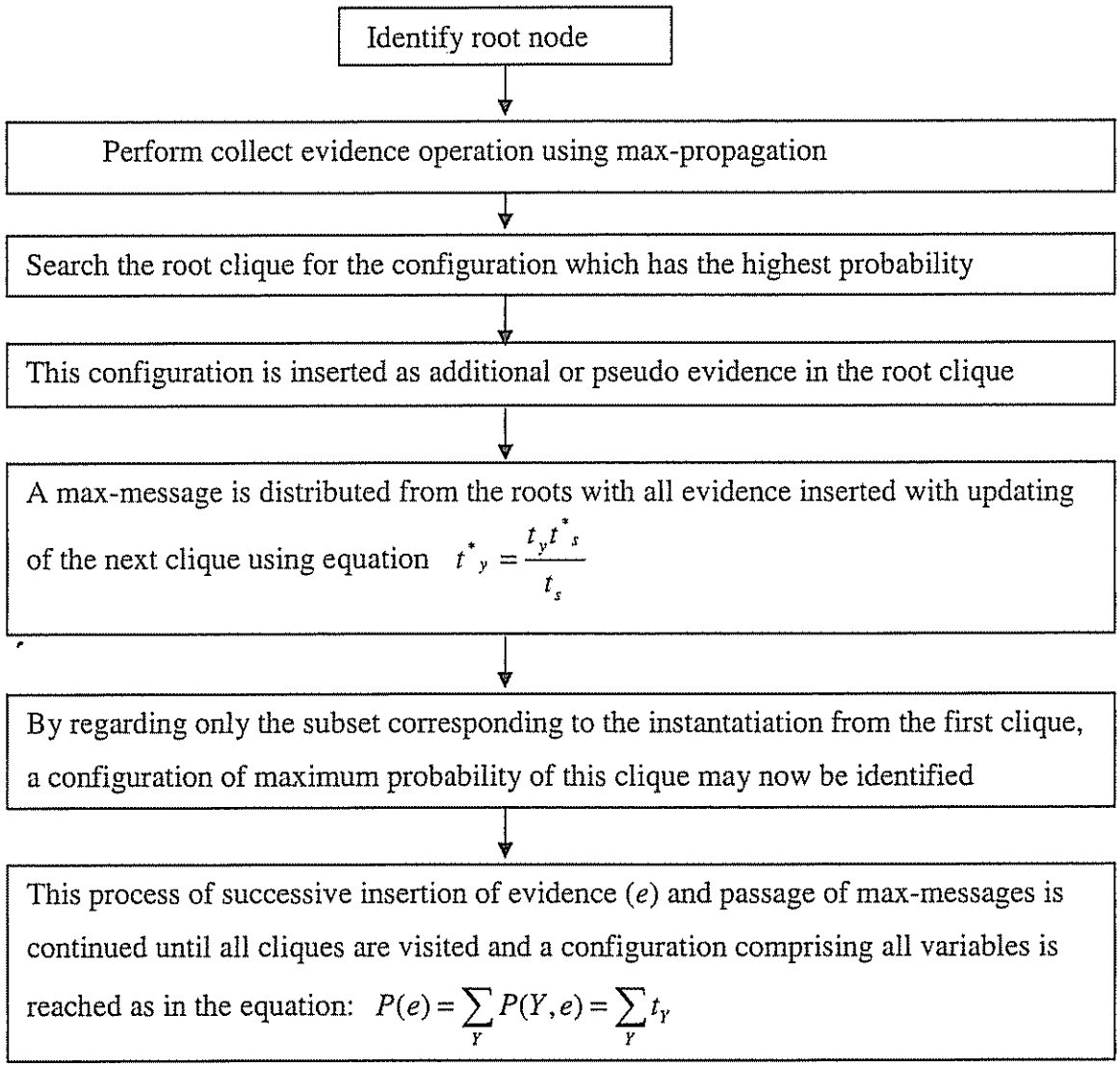

Fig. 2.24 Procedure for determining the most probable configuration (Madsen and Jensen, 1999/ Friis-Hansen, 2000)

Next, obtain the second most likely configuration by inserting pseudo-evidence and subsequent max-propagation. This defers from the most likely configuration in at least one of the variables. The mode of carrying this out is shown in figure 2.25.

Insert pseudo-evidence that the state of the first variable, X_1 is not in the configuration of maximum probability i.e. $X_1 = c_1 *$.Next, carry out max-propagation to identify the most probable configuration with this pseudo-evidence.

↓

Insert pseudo-evidence so that $X_1 = c_1 * \wedge X_2 \neq c_2 *$, here the first variable (X_1) is in a state of maximum probability while the second (X_2) is not.

↓

Repeat this max-propagation N_v times to give pseudo-evidence of the max-configuration M_1 on all variables except the N_v'th one, $X_1 = c_1 * \wedge X_2 = c_2 * \wedge \ldots \wedge X_{N_{v-1}} = c_{N_{v-1}} * \wedge X_{N_v} \neq c_{N_v} *$ which are N_v configurations ≡the second most probable of the joint distribution
By applying the equation: $P(e) = \sum_Y P(Y, e) = \sum_Y t_Y$ to all N_v configurations, the probability of each is obtained and the second most likely is found.

Fig. 2.25 Determination of the second most likely configuration (Madsen and Jensen, 1999/ Friis-Hansen, 2000)

2.8.4 Correlation

Covariance in Bayesian networks is calculated from the conditional probability distribution for two variables X and Y as shown below (Friis-Hansen, 2000):

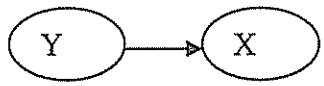

Fig. 2.26 Illustration of covariance between two variables

$$\text{Cov(X,Y)} = \text{E[XY]} - \text{E[X]}\,\text{E[Y]} = \sum_{i=1}^{N_1^X}\sum_{j=1}^{N_1^Y} P(x_i, y_j)x_i, y_j - (\sum_{i=1}^{N_1^X} P(x_i)x_i)(\sum_{j=1}^{N_1^Y} P(y_j)y_j)$$

$$= \sum_{i=1}^{N_1^X} x_i \sum_{j=1}^{N_1^Y} P(x_i|\ y_i)P(y_j)y_j - (\sum_{i=1}^{N_1^X} P(x_i)x_i)(\sum_{j=1}^{N_1^Y} P(y_j)y_j)$$

$$= \sum_{i=1}^{N_1^X} x_i \sum_{j=1}^{N_1^Y} P(x_i|\ y_j)P(y_i)y_j - (\sum_{i=1}^{N_1^X} P(x_i)x_i)(\sum_{j=1}^{N_1^Y} P(y_j)y_j)$$

where N_1^X and N_1^Y – number of states in variable X and Y respectively and

$P(x_i) = \sum_{j=1}^{N_1^Y} P(x_i|\ y_j)P(y_j)$ is the marginal distribution P(X)

2.8.5 The Concept of Directional (D) Separation

This is a characteristic of directed graphs which may be exploited to identify irrelevant information in a Bayesian network or influence diagram. Two nodes of a Bayesian Network are said to be d-separated if they are conditionally independent given a specified set of nodes. If $P(A|B,C) = P(A|C)$ then A and B are conditionally separated given C.

Hence, the different types of connections present in a directed graph as:

i) Serial connection ($A \rightarrow B \rightarrow C$): Evidence is transmitted from A to B only if C is not in a specific state or instantiated.
   If C is instantiated, then A and B are conditionally independent given C

ii) Diverging connection ($A \leftarrow B \rightarrow C$): Evidence is transmitted through C if it is not instantiated. A and B are then d-separated given C.

iii) Converging connections ($A \rightarrow B \leftarrow C$): A and B are independent if nothing is known about C. However, knowledge of C enables information to be transmitted from A and B therefore making conditionally dependent given C.

A path is active when every vertex on the path is active. Paths and vertices on these paths are active or inactive relative to a set of other vertices Z.

Example:

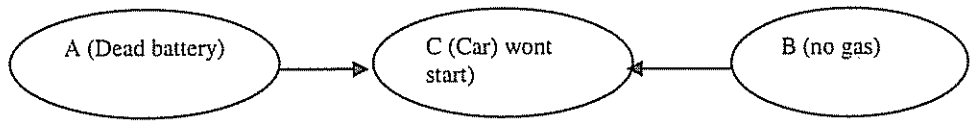

Fig. 2.27 Illustration of the concept of d-separation (Bishop, 2002)

Consider an example in which there are two independent causes of a car refusing to start namely having 'no gas' and having a 'dead battery'. Evidence that the battery is charged after observation that the car won't start tells me that the gas tank must be empty. So, the independent causes are made dependent by conditioning on a common effect.

Chapter 3: Formulation of the Model

3.1 Introduction

The model that was developed for determining the response of a typical embankment is shown in figure 3.1. It consists of a module within which the variables that influence the critical embankment characteristics represented by four nodes namely the temperature, leachate concentrations, horizontal pressures and settlements are analysed. The outputs from these nodes can then be compared with the analysis results of data obtained from the sensors in the field. Thereafter, the level of risk can then be obtained for the particular embankment.

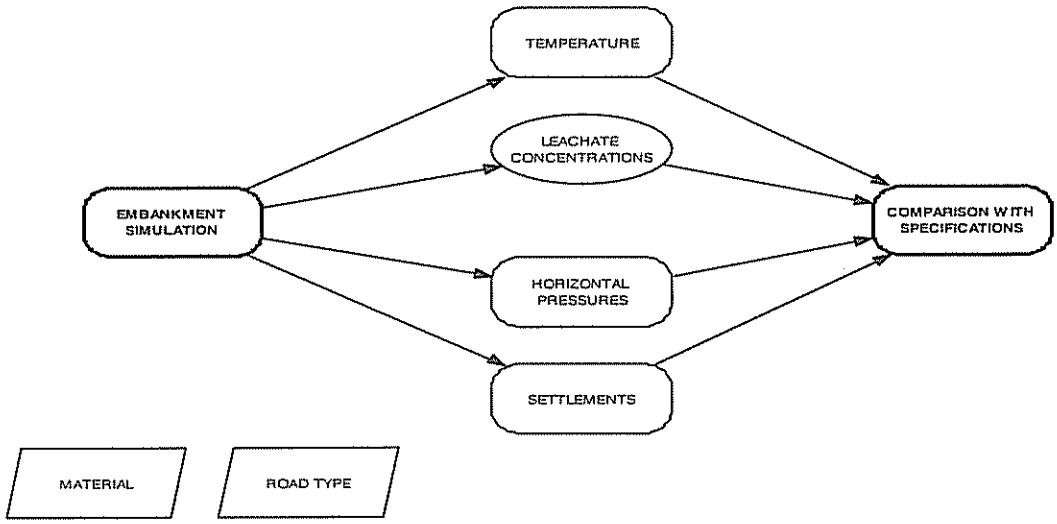

Fig. 3.1 Model for Embankment Simulation

3.2 Development of the junction tree for the model

Even though the analysis is carried out using a computer program, the junction tree shows how information is updated in the network. The junction tree for figure 3.1 is formed as follows;

Let T represent Temperature

L represents 'Leachate Concentrations' node

H represents 'Horizontal pressures' node

S represents 'Settlement' node

E represents set of variables under 'embankment simulation node

C represents set of variables under 'comparison with specifications' node

a) Moralize the graph (figure 3.2)

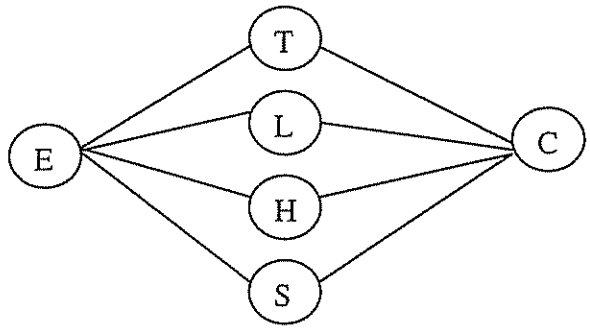

Fig. 3.2 Moralized graph

b) Triangulate the graph and eliminate node C so that the number of cliques should be minimized (figure 3.3)

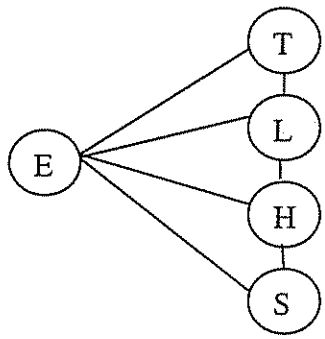

to form clique {C,T,L,H,S}

Fig. 3.3 First step in triangulating the graph

c) Triangulate the graph again and eliminate node E (figure3.4)

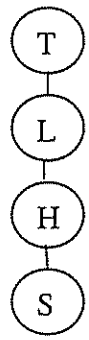

to form clique {E,T,L,H,S}

Fig. 3.4 Second step in triangulating the graph

the junction tree formed is shown in figure 3.5:

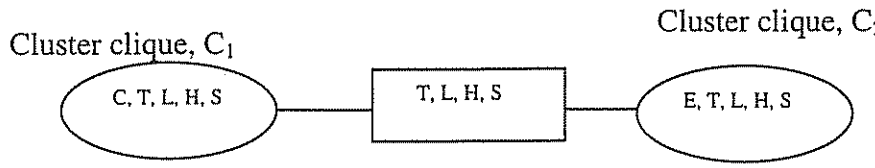

Fig. 3.5 Junction tree

3.3 Model Inputs

The input variables for the embankment characteristics are analyzed under the 'embankment simulation' module:

3.3.1 Temperature

In order to model the embankment temperatures, the variables considered are shown in figure 3.6.

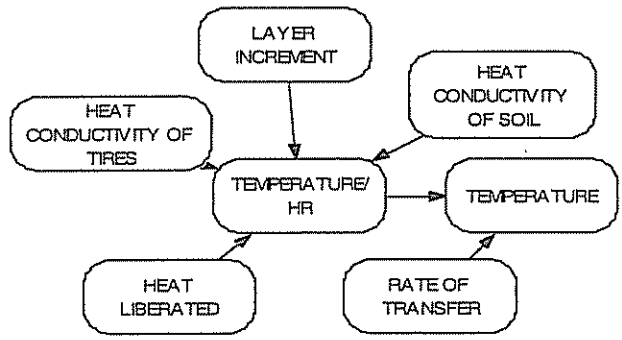

Fig. 3.6 Diagram Illustrating the Temperature Response of the Embankment

Each variable depends on particular mathematical expressions/values as follows:

- Heat conductivity of tires (H_{ct}) - 0.086 W/mK
- Heat conductivity of soils (H_{cs}) - a value between 1 and 100 W/mK is recommended
- Layer increment (Li) - this varies between 0 and 5.49m which is the full height of the embankment
- Heat liberated (H_l) – a value of 1 W/hr is used in this case (Shalaby 2005)
- Rate of transfer (Rot) through the fill – 1.05%

- The temperature per hour (Tphr) flowing through the embankment is determined using the variables above and the 'if statement' program as follows:
  IF Li < 3.05 and Li >3.965 THEN $H_l/(H_{ct}*(5.49-Li))$ *ELSE* $H_l/(H_{cs}*(5.49-Li))$
- The temperature response is then obtained by using the dynamic command as follows:

  *Dynamic(Tphr,T[Time-1]*Rot)*

The dynamic simulation calculates the value of the variable at each element of time.

3.3.2 Leachate characteristics

The model for the leachate characteristics of the embankment was developed based on the observed maximum leachate response of scrap tire fills as studied by Humphrey (2000) at four major locations in the US and as documented in the ASTM D6270 (1998). The values are random and hence are represented by a normal distribution as follows:

- pH - mean value of 6.9 and standard deviation of 0.5
- Cadmium - mean concentration of $5x10^{-5}$g/l and standard deviation of $9.86x10^{-6}$g/l
- Lead - mean concentration of $1.5x10^{-5}$g/l and standard deviation of $6.94x10^{-5}$g/l
- Chromium - mean concentration of $1x10^{-4}$g/l and standard deviation of $1.38x10^{-4}$g/l
- Selenium - mean concentration of $5x10^{-4}$g/l and standard deviation of $2.88x10^{-5}$g/l
- Zinc - mean concentration of $5x10^{-3}$g/l and standard deviation of $1.51x10^{-3}$ g/l
- Chloride - mean concentration of $2.5x10^{-4}$g/l and standard deviation of $2.50x10^{-5}$g/l
- Sulphate - mean concentration of 0.25g/l and standard deviation of 0.14g/l
- Aluminium - mean concentration of $1.250x10^{-4}$g/l and standard deviation of 0.07g/l
- Iron - mean concentration of $3x10^{-4}$g/l and standard deviation of 94.08 g/l
- Manganese - mean concentration of $5x10^{-5}$g/l and standard deviation of $1.62x10^{-3}$ g/l

Figure 3.7 shows the model that was developed to simulate the leachate concentrations of the embankment.

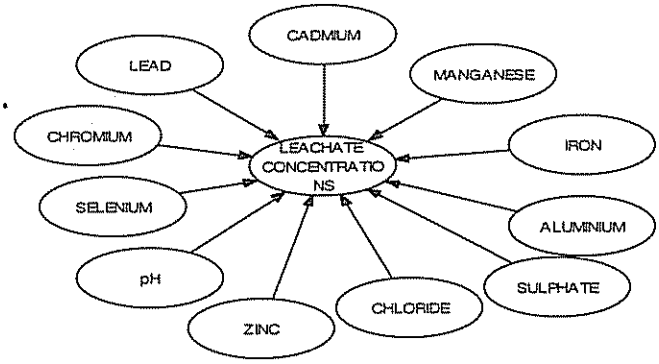

Fig. 3.7 Diagram Illustrating the Leachate Model for the Embankment

3.3.3 Settlements:

The settlement response of the embankment was simulated using the influence diagram in Figure 3.8.

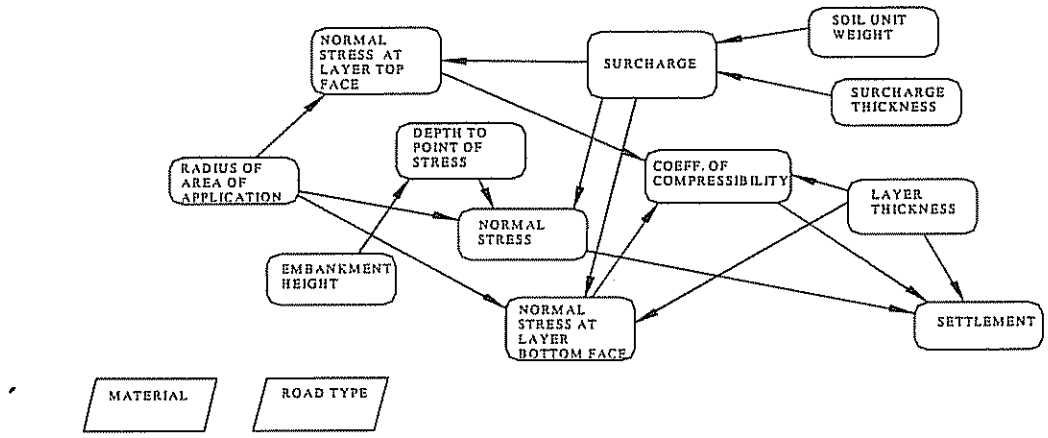

Fig. 3.8 Diagram Illustrating the Settlement Model for the Embankment

The major factors considered and the underlying variables are as follows:

- Surcharge unit weight which is considered to be a layer of soil placed on the surface of the embankment immediately after construction to accelerate the settlement process. The soil unit weight depends on the type of traffic the pavement is designed for and also whether the road is paved or not. Typical values considered are shown on table 3.1.

Table 3.1 Surcharge Unit Weights

Type of Traffic	Soil unit weights (kN/m^2)
Heavy traffic (paved roads)	24
Low traffic (paved roads)	9.6
All traffic types (unpaved roads)	6
No surcharge	0

- Normal stresses (σ) at the point where the settlement is of interest. This was obtained using the Boussinesq's equation :

$$\text{Normal stress, } \sigma = \textit{Surcharge load} \times (1-(z^3/(R^2+z^2)^{1.5}))$$

where z – depth to stress point within embankment

R – radius of application of surcharge

- Coefficient of compressibility of the embankment layer given by the equation:

$$C_c = h/(\sigma_1 - \sigma_2)$$

where z – embankment layer thickness

σ_1, σ_2 – normal stress at top and bottom surface of layer under investigation

- Other variables considered are the layer thickness, embankment height
- Settlement is given by the equation: $S = C_c \times H \times (\sigma)$

3.3.4 Horizontal pressures

The horizontal pressure in the embankment was simulated using the influence diagram in Figure 3.9

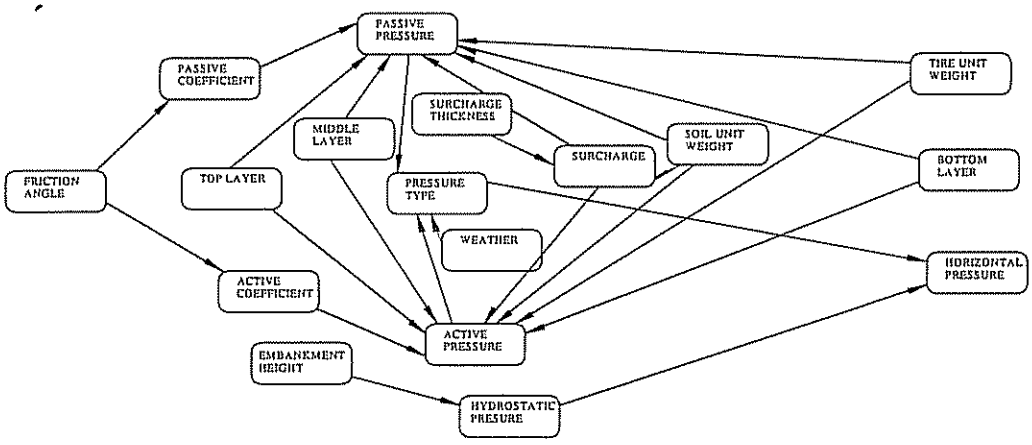

Fig. 3.9 Diagram Illustrating the Horizontal Pressure Model for the Embankment

The horizontal pressures exerted by the embankment on the abutment wall of the integral abutment bridge are modeled as passive pressure during the hot season and active pressure during the cold season. The general variables considered in constructing the model for the horizontal pressures are:

Friction angle, Layer increment and Surcharge

- Type of climate; (hot or cold)

For the passive pressures, the specific variables considered are:

- Coefficient of passive earth pressure given by the equation:

  $K_p = (1 + \sin(\phi))/(1 - \sin(\phi))$ *and*

- the passive earth pressure is obtained using the equation:

  $P_p = K_p(\gamma_s h_s + \gamma_{t1} h_1 + \gamma_{t2} h_2 + q) + \gamma_w h_w$

For the active pressures, the specific variables considered are:

- Coefficient of active earth pressure given by the equation:

  $K_a = (1 - \sin(\phi))/(1 + \sin(\phi))$

- the passive earth pressure is obtained using the equation:

  $P_a = K_a(\gamma_s h_s + \gamma_{t1} h_1 + \gamma_{t2} h_2 + q) + \gamma_w h_w$

where γ_s = unit weight of sand ; γ_{t1} = unit weight of top tire layer

γ_{t2} = unit weight of bottom tire layer ; h_2 = unit weight of sand

q = surcharge ; γ_w = unit weight of water

h_w = head of water

3.3.5 Model Outputs

The output variables that determine the characteristics of the embankment are analyzed by the sub-model shown in figure 3.12 under the 'comparison with specifications' module. The variables labeled MEAN and STDDEV give the average and standard deviation of the random values of the corresponding characteristics. The 'distribution' nodes convert the mean and standard deviations calculated into probability distributions that best represent them while the nodes labeled 'max' run a query through the each set of distribution to identify the maximum probability density. The index nodes LT, Pd, SETTLEMENT and CHARACTERISTICS specify the labels for the depths, probability density, settlements and the leachate properties respectively. The nodes

labeled CO1, CO2, CO3 and CO4 the maximum probability density of each simulated characteristic with that measured in the field while the RISK LEVEL node gives the condition of the embankment using a 'SAFE' or 'FAIL' criterion.

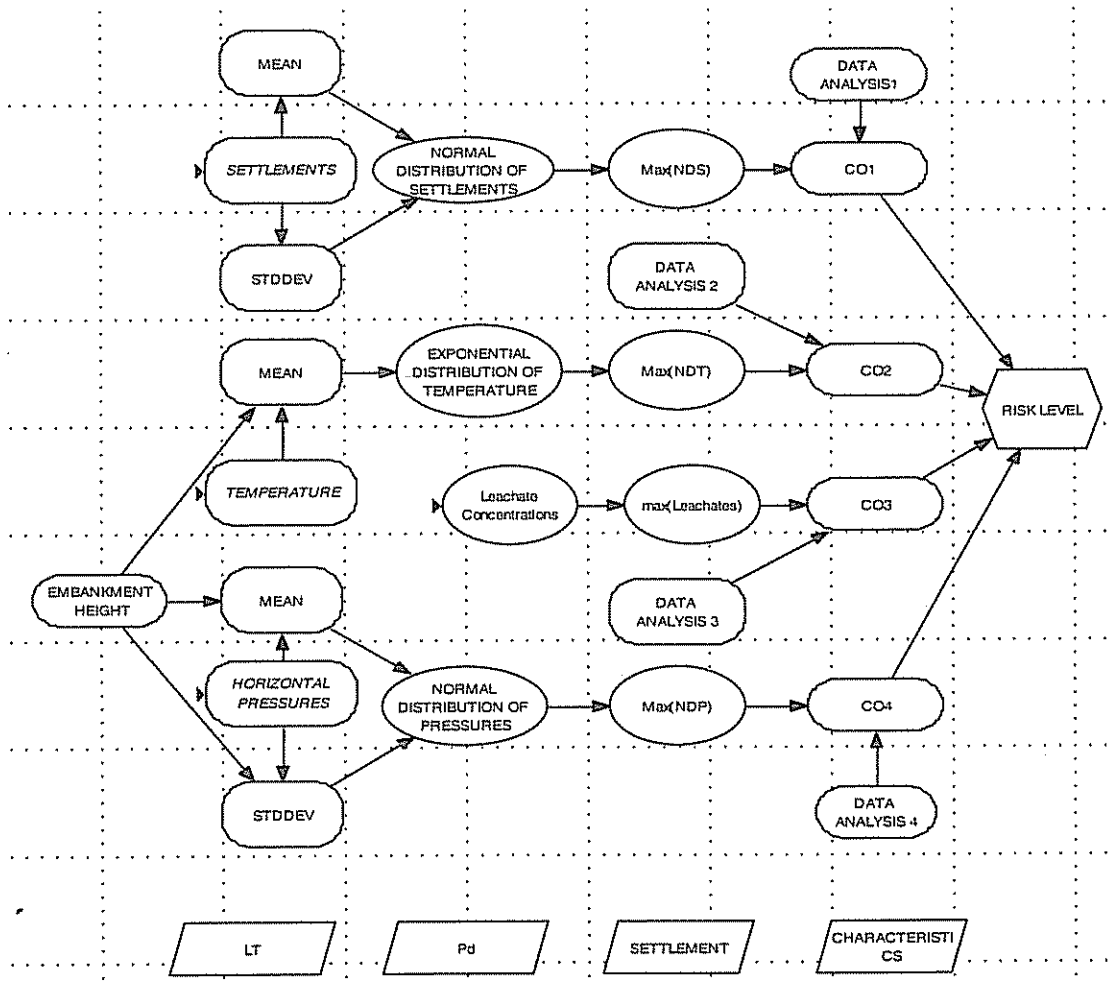

Fig 3.10 Diagram Illustrating the Output Model

The sub-model then compares the maximum probability density of the embankment materials corresponding to the particular characteristic of settlements, temperature or horizontal pressure with that obtained from analysis of data obtained from the field. The output specifies a failure if the latter exceeds the former. In the case of the leachates, the maximum concentrations computed for the embankment based on literature are used as the limiting criteria.

Chapter 4: Analysis and Interpretation of Data

4.1 Data Analysis

4.1.1 Temperature Response

The temperature response of the embankment down its depth based on the input variables is as shown in figure 4.11:

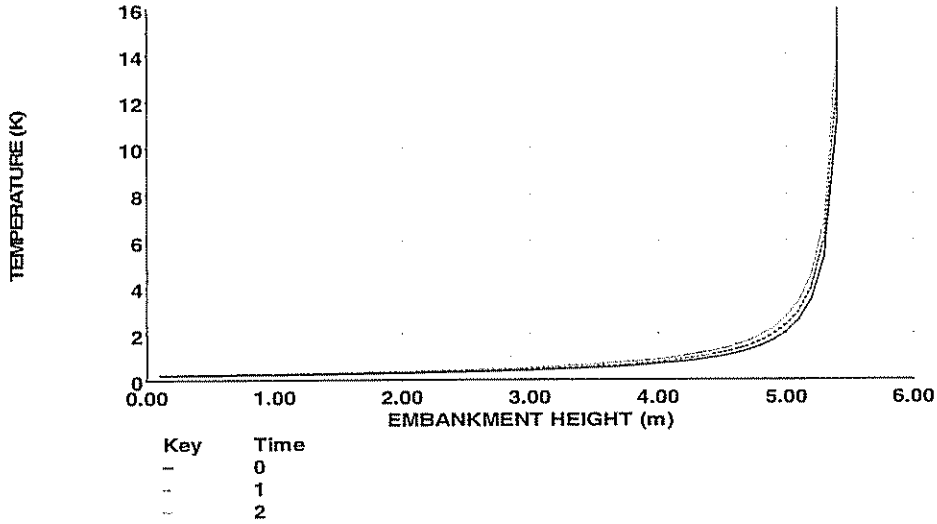

Fig. 4.11 Temperature Response against depth

Figure 4.12 shows the variation of temperature with time at different depths within the embankment.

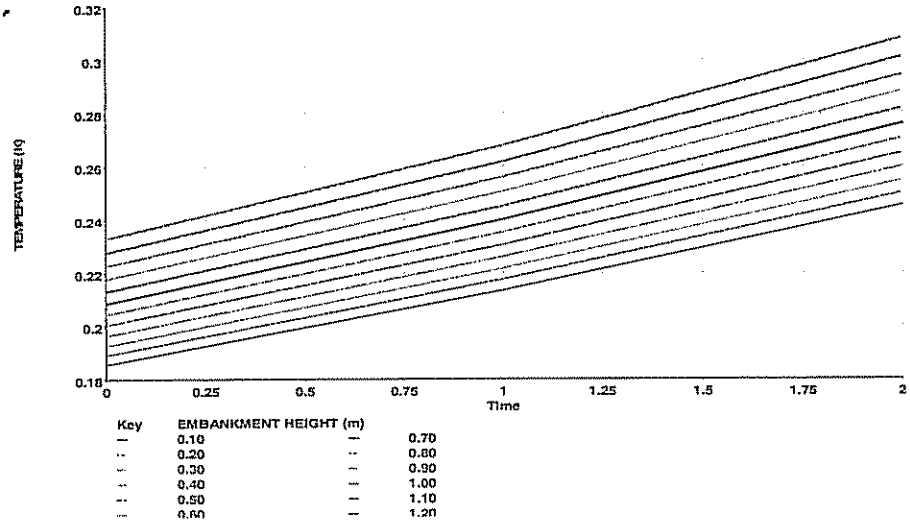

Fig. 4.12 Temperature Response against time

The probability distribution of the temperature response in time is then obtained in form of an exponential distribution as shown in figure 4.13

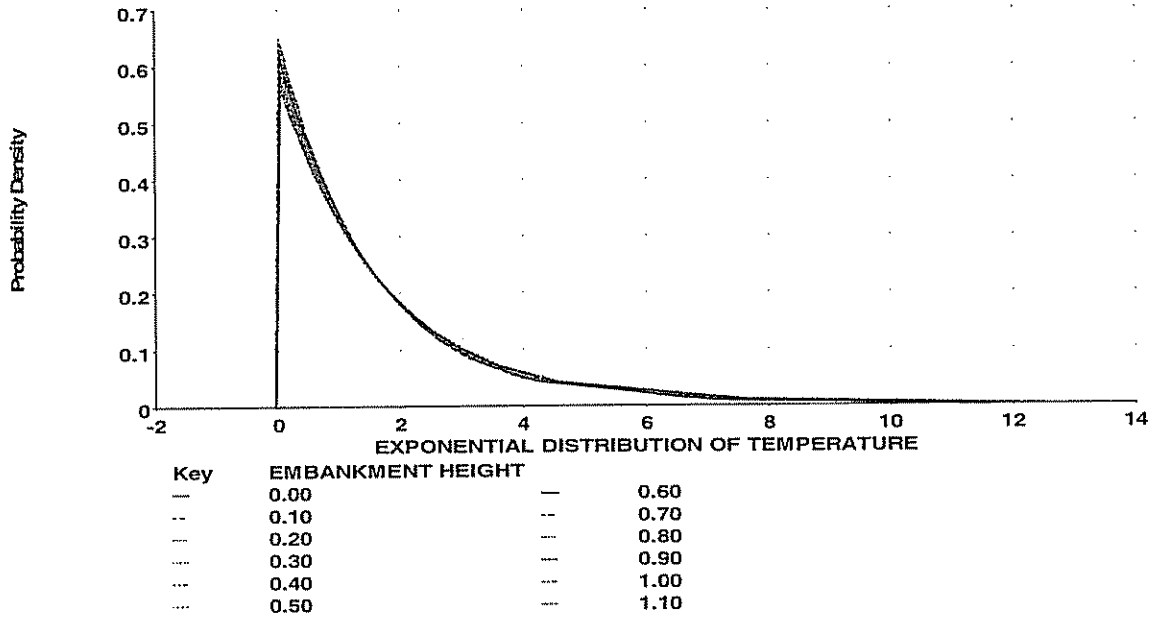

Fig. 4.13 Exponential distribution of the temperature response

4.1.2 Leachate Characteristics

Table 4.2 shows the limiting leachate characteristics for a typical scrap tire embankment based on literature.

Table 4.2 Distribution of Leachate Characteristics in Embankment

	Min	Median	Mean	Maximum	Std. Dev.
Lead	-1.640×10^{-4}	1.500×10^{-5}	1.500×10^{-5}	1.940×10^{-4}	6.939×10^{-5}
Zinc	1.108×10^{-3}	5.000×10^{-3}	5.000×10^{-3}	8.892×10^{-3}	1.509×10^{-3}
Cadmium	-2.042×10^{-5}	5.000×10^{-6}	5.000×10^{-6}	3.042×10^{-5}	9.857×10^{-6}
Selenium	4.256×10^{-4}	5.000×10^{-4}	5.000×10^{-4}	5.744×10^{-4}	2.883×10^{-5}
Chromium	-2.552×10^{-4}	1.000×10^{-4}	1.000×10^{-4}	4.552×10^{-4}	1.377×10^{-4}
Aluminium	-0.1747	1.250×10^{-4}	1.250×10^{-4}	0.1749	0.06778
Chloride	1.856×10^{-4}	2.500×10^{-4}	2.500×10^{-4}	3.144×10^{-4}	2.497×10^{-5}
Sulphate	-0.1175	0.25	0.25	0.6175	0.1425
Manganese	-4.126×10^{-3}	5×10^{-5}	5×10^{-5}	4.226×10^{-3}	1.619×10^{-3}
Iron	-242.7	3×10^{-4}	3×10^{-4}	242.7	94.08
pH	5.612	6.9	6.9	8.188	0.4993

4.1.3 Settlement response:

The relative settlement response within the embankment at different depths based on the input variables is as shown in figure 4.14.

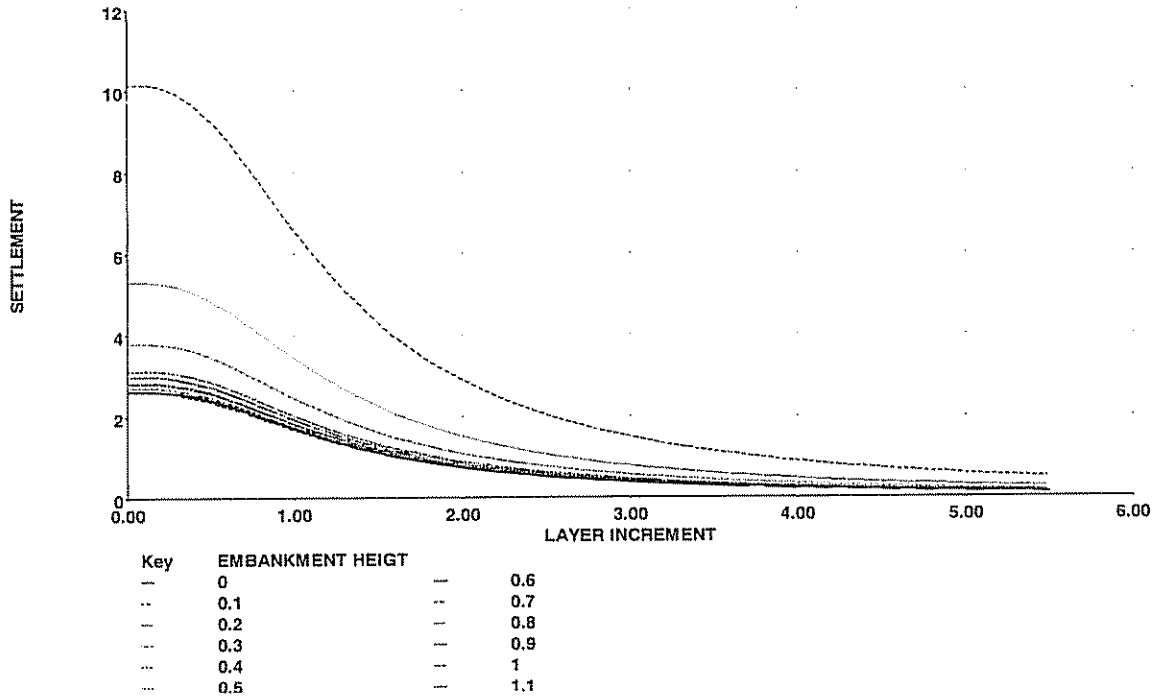

Fig. 4.14 Settlement Response against depth

Settlements at different depths are represented by different broken lines as shown in the key. The most prominent of these is the one indicating settlements at a depth of 0.1m into the embankment. Others are also indicated at intervals of 0.1m from one another. The largest settlement of 10.15cm occurs at the depth of 0.1m while the settlements at other depths are relatively smaller.

The normal distribution of the relative settlements at different depths in the embankment is obtained as shown in figure 4.15. It shows that the normal distribution of settlements at a depth of 0.1m has a lower peak than the settlements at other depths. The settlements at a depth of 0.7m however give a probability density that has the highest peak of 0.492.

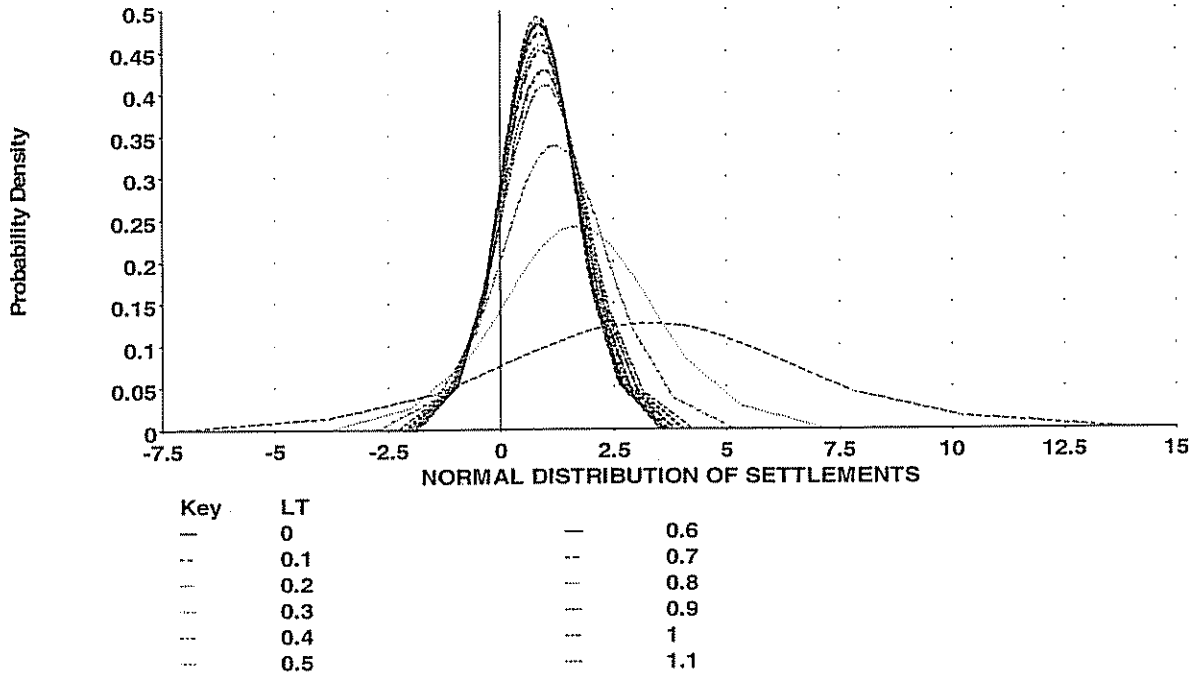

Fig. 4.15 Normal distribution of the relative settlements

4.1.3 Horizontal pressure responses:

The horizontal pressures developed within the embankment under the two climatic conditions are as shown in figures 4.16a and 4.16b.

a) In cold climate:

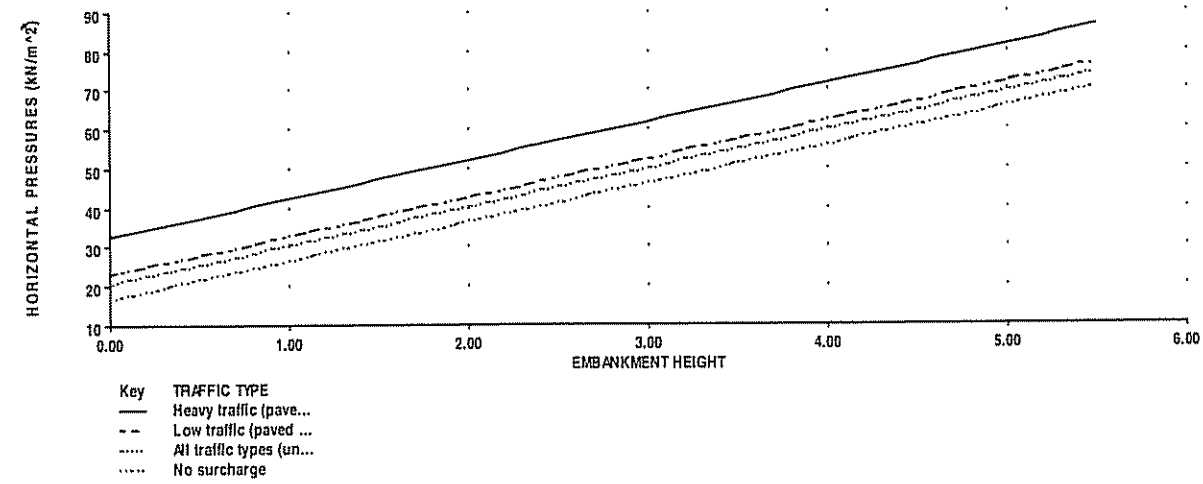

Fig. 4.16a Horizontal Pressure Response

b) In hot climate:

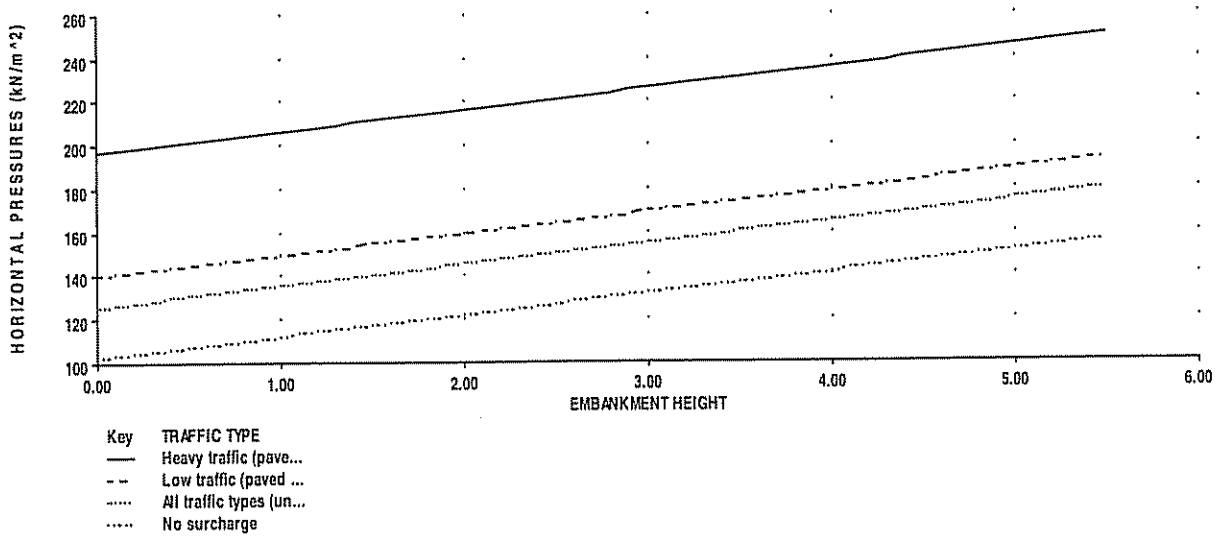

Fig. 4.16b Horizontal Pressure Response

Figures 4.16a and b agree well with the fact that a higher horizontal pressure should result from a higher surcharge load hence the load due to heavy traffic produces the highest horizontal pressure while the case in which no surcharge is applied produces the lowest pressure. Figure 4.17 shows the normal distribution of horizontal pressures varying between the two climatic conditions.

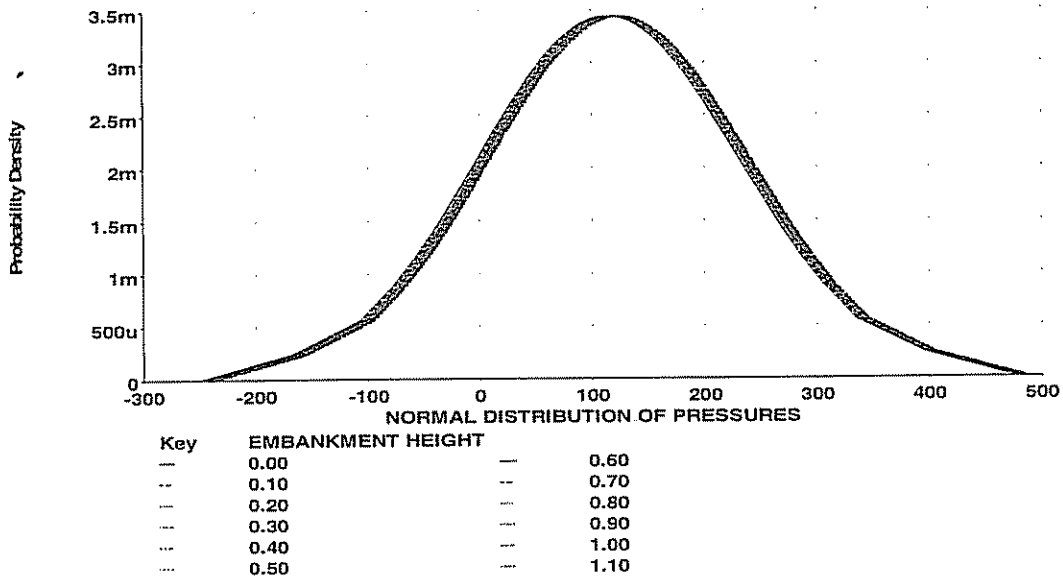

Fig. 4.17 Normal distribution of the horizontal pressures

The normal distributions of the horizontal pressures in figure 4.17 are very close because the relative differences between the pressures under the cold and hot conditions at different depths are very close.

4.2 Interpretation of Results

The variation of temperature within the embankment with depth at any particular point in time is measured in hours (figure 4.11). It is observed that the temperature in the embankment increases uniformly (that is, exponentially) with the depth (measured at intervals of 0.1m) of the embankment even though there is a transition in materials at depths of 3.05m and 3.965m.

Figure 4.12 shows that the temperature increases at any particular depth within the embankment varies linearly with time. The straight line occurring in Figure 4.13 at the zero temperature mark is due to the fact that the corresponding exponential of the zeros in the temperature data equal one while probability distributions for negative temperatures are positive. Figure 4.13 also shows that a greater proportion or density of the embankment is at lower temperature at the surface than further within it. For the embankment considered, the overall maximum probability density obtained for the temperatures is 0.9703.

Table 4.2 shows the desirables concentration limits for leachates from the embankment within which measured values may fall without any harmful consequences. The maximum levels for the leachate characteristics as computed by the model are shown in Table 4.2.

Figure 4.14 shows the simulated relative settlements at different depths (0.1m apart) within the embankment. At any particular depth, the relative settlements of points within the embankment measured at 0.1m intervals decrease the further into the embankment the settlement is observed. On the other hand, the overall settlement varies non-uniformly from one layer to the other.

Figure 4.15 shows that a smaller proportion or density of the embankment experiences higher settlements the nearer the surface of the embankment it is than the proportions further within. Considering the embankment particles at a depth of 0.1m, the corresponding settlement of 10.15cm and probability density of 0.126 were recorded

while those at a depth of 1.1m have a corresponding settlement of 2.987cm and density of 0.428. For the embankment considered, the overall maximum probability density obtained for the settlements is 0.492.

Figures 4.16a and b show the variation of lateral pressures with depth for the different traffic types under cold and hot climates respectively. It is observed that in both cases, the pressures increase linearly with depth through the embankment. Figure 4.16a shows that the pressures developed within the embankment and acting on the abutment under a cold climate are active whereas figure 4.16b shows that the pressures developed under the hot climate are passive. The active pressures are much lower than the passive pressures. For the embankment considered, the overall maximum probability density obtained for the horizontal pressures (figure 4.17) is 0.00344.

- The temperature profiles down the embankment due to variations at any depth other than at the surface are similar and this is evident from the fact that their probability distribution curves have similar gradients. For any two or more points at different depths within the embankment, the temperature across the embankment section does not vary. This means that only a few sensors are required to study temperature variations within a scrap tire embankment. In addition, it is very unlikely that temperature variations within an embankment of similar geometry on site could pose any reasonable risk considering that the maximum probability density for the simulated temperatures is considerably high (0.9301).
- Since the relative settlements are highest near the surface of the embankment (10.15cm) and the corresponding density of the tire shred materials is lowest here (0.126), very sensitive sensors will be required at these locations to capture the settlement information. At points further within the embankment such as at a depth of 1.1m where the corresponding density of material under deflection is greater (that is, 0.428) and the settlement is lower (2.987cm), the information can be easily obtained by sensors functioning reasonably well.
- The horizontal pressures under a hot climate should be considered critical when designing the abutment wall since they are greater in magnitude than the horizontal pressures under a cold climate. The resulting normal distributions of pressures at different depths within the embankment are similar and the peaks occur at an average pressure corresponding to a depth of 5.49m that is, the bottom of the embankment. The temperature conditions under which the model is analyzed for horizontal pressures should be further varied to consider how other intermediate temperatures affect the pressures. Further studies into how this aspect of the model can be developed to analyze horizontal pressures at different temperatures will be required. This will help to produce distinct differences between the normal distributions of the horizontal pressures and ensure better interpretation of the results.
- The characteristics of the embankment which require critical assessment are the settlement and horizontal pressures because their corresponding maximum

probability densities simulated by the model are considerably low at 0.428 and 0.0034 respectively.

- The three characteristics of the embankment namely the temperature, horizontal pressure and settlements should be analyzed using the model and varying thicknesses of sand layer to check if their distribution across the sand-tire transition will remain uniform with a sand layer thicker than 3 feet (0.915m).

References

- Analytica® Software: Analysis Tools. Lumina Decision Systems Inc., 26010 Highland Way, Los Gatos CA 95033-9758, USA, 2006.
- Baker T. E., Allen T. M. and Pierce L. M. (2003) "Evaluation of the Use of Scrap Tires in Transportation related applications in the State of Washington" Washington State Department of Transportation.
- Bayraktarli Y. Y., Ulfkjaer J., Yazgan U. and Faber M. H. (2005) On the Application of Bayesian Probabilistic Networks for Earthquake Risk Management. Proceedings Paper presented at the 9th International Conference on Structural Safety and Reliability, Rome, Millpress, Rotterdam, 40(4), 3505-3512.
- Bishop C. M. (2002) " Probabilistic Graphical Models" Lecture on Graphs and Markov Properties delivered at NATO Advanced Study Institute Conference.
- Cecich V., Gonzales L., Hoisaeter A., Williams J. and Reddy K. (1996) "Use of Shredded Tires as Lightweight Backfill Material for Retaining Structures". Waste Management and Research J.14, 433 - 451.
- Chu C. (1998) "A Geotechnical Investigation of the Potential Use of Shredded Scrap Tires in Soil Stabilization". A Dissertation Submitted to Kent State University in partial fulfillment of the requirements for the degree of Doctor of Philosophy.
- Chung K. and Hong Y. (2002) "Scrap Tire Aggregate Composite: Composition and Primary Characterization for Pavement Material ". Polymer Composites. 23(5), 852-857.
- Clescerl L. S., Greenberg A. E., Eaton A. D. (1999) "Standard Methods for Examination of Water & Wastewater". 20th Edition American Public Health Association (APHA).
- Edil T. B., Park J. K., Kim J.Y. (2004) "Effectiveness of Scrap Tire Chips as Sorptive Drainage Material". Journal of Environmental Engineering (ASCE). 130(7), 824-831.
- Friis-Hansen A.(2000) "Bayesian Networks as a Decision Support Tool in Marine Applications" A Dissertation Submitted to the Department of Naval Architecture and Offshore Engineering, Technical University of December in partial fulfillment of the requirements for the degree of Doctor of Philosophy.

- Garga V. K. and O'Shaughnessy (2000). "Tire Reinforced Earthfill, Part 1: Construction of a Testfill Performance and Retaining Wall Design". Canadian Geotech. J., Canada. 37, 75-96.
- Grimes B. H., Steinbeck S. and Amoozegar A. (2003) "Analysis of Tire Chips as a Substitute for Stone Aggregate in Nitrification Trenches of Onsite Septic Systems: Status and Notes on the Comparative Microbiology of Tire Chip Versus Stone Aggregate Trenches" Small Flows Quarterly. 4(4), 18-21.
- Hao D. (2000) Application of Influence Diagram and Sequential Hypothesis Testing Method in Bridge Maintenance Decision Making. MTC Transportation Scholars Conference Ames, Iowa.
- Hoppe E. J. and Mullen W. G. (2004) "Final Report Field Study of a Shredded-tire Embankment in Virginia" Virginia Transportation Research Council. Charlottesville, Virginia. 4(20).
- Humphrey D. N. and Katz L. E. (2000) "Five-Year Field Study of the Water Quality Effects of Tire Shreds placed above the Water Table". 79th Annual Meeting of the Transportation Research Board, Washington, D.C. No. 00-0892
- Humphrey D. N. and Katz L. E. (2001) "Field Study of Water Quality Effects of Tire Shreds Placed Below the Water Table". Proceedings of the International Conference on Beneficial Use of Recycled Materials in Transportation Applications, Arlington.699-708.
- Humphrey D. N. and Tweedie J.J. (2002) "Tire Shreds as Lightweight Fill for Retaining Walls- Results of Full Scale Field Trials". Proceedings of the workshop on lightweight Geomaterials, Tokyo, Japan.
- Humphrey D. N., Fiske A. J.and Eaton R. A. (2002) "Backcalculation of Tire Chips from instrumented Test Section" 81st Annual Meeting of the Transportation Research Board, Washington, D.C.
- Humphrey D. N., Whetten N., Weaver J., Rocker K. (2000)"Tire shreds as lightweight fill for construction on weak marine clay" Proceedings of the International Symposium on Coastal Geotechnical Engineering in Practice, Balkema, Rotterdam. 611-616.

- Humphrey D.N. (2003) "Civil Engineering Applications of Scrap Tires. California Integrated Waste Management Board.
- Humphrey D.N. and Blumental M (1998) "Civil Engineering Applications of Scrap Tires: An Emerging Market". Resource Recycling Portland.
- Jensen F. V. (2002) "Bayesian Networks and Decision Graphs (Statistics for Engineering and Information Science)".Springer-Verlag, New york.
- Jensen, F. V. (1995), "Cautious Propagation in Bayesian Networks'. Proceedings of the 11th Conference on Uncertainty in Artificial Intelligence, Montreal, Canada, 323-328.
- Kjærulff U. B. and Madsen A. L. (2005) Probabilistic Networks - An Introduction to Bayesian Networks and Influence Diagrams. Aalborg University.
- Lawrence, B., Humphrey, D.N., Chen, L. (1999) "Field Trial of Tire Shreds as Insulation for Paved Roads", Proceedings of the Tenth International Conference on Cold Regions.
- Li G., Stubblefield M. A., Garrick G., Eggers J., Abadie C., Huang B. (2004) "Development of Waste Tire Modified Concrete ". Cement and Concrete Research. 34(12), 2283-2289.
- Madsen A. L. and Jensen F. V. (1999) "Lazy Propagation: A Junction Tree Inference Algorithm Based on Lazy Evaluation" Journal of Artificial Intelligence J. 113, 203-245.
- Maryland Department of the Environment (2005). "Scrap Tire Recycling"
- McKenzie C.M. (2003). "Use of Scrap Tires as Aggregate in Soil Absorption Systems". Small Flows Quarterly, 4(4), 14-17.
- Moo-Young, Sellasie K.Zeroka D., Sabnis G. (2003). "Physical and Chemical Properties of Recycled Tire Shreds for Use in Construction". J. of Environmental Engineering (ASCE). 129(10), 921-929.
- Pfeiffer D. U.(1997) "Decision Analysis and Risk Analysis". Risk Analysis and Animal Health Manual, International Training Course, Switzerland. 861 – 877.
- Pierce C.E. and Blackwell M. C. (2002) "Potential of Scrap Tire Rubber as Lightweight Aggregate in Flowable Fill" Waste Management J. 23, 197-208.

- Rubber Manufacturers Association (2005) "Scrap Tires" Proceedings of the International Symposium on Coastal Geotechnical Engineering in Practice, Balkema, Rotterdam. 611-616.
- Shachter R. D. Probabilistic Inference and Influence Diagrams. Operations Research Journal, Vol. 36, No. 4, 1988.
- Shalaby A. and Khan R. A. (2005) "Design of Unsurfaced Roads Constructed with Large-Size Shredded Rubber Tires: A Case Study ". Resources Conservation and Recycling. 44(4), 318-332.
- Siddique R. and Naik T. R. (1995) "Properties of Rubberised Concrete".Int. J. of Integrated Waste Management, Science and Technology. 25(2), 304 - 310.
- Topcu I. B (1995) "The properties of Rubberised Concrete" Cement and Concrete Research, Vol. 25. No. 2. pp. 304-310.
- Yang S. , Kjartanson B. H. , and Lohnes R. A. (2001)"Structural performance of scrap tire culverts" Can. J. Civ. Eng. 28, 179 -189.
- Yang S., Lohnes R. A. ,Kjartanson B. H. (2002) "Mechanical Properties of Scrap Tires". Geotech. Testing J. 25(1), 44 - 52.
- Youwai S., Bergado D. T. (2003) "Strength and Deformation Characteristics of Shredded Rubber Tire –Sand Mixtures". Canadian Geotech. J. 40, 254 - 264.
- Youwai S., Bergado D. T. (2004) "Numerical Analysis of reinforced wall using rubber tire chips-sand as backfill material". Computers and Geotech. J. 31, 103 - 114.
- Zvanut P. (2003) "Settlements of an Embankment founded on a Soft Soil". Proceedings of the 11th FIG Symposium on Deformation Measurements, Santorini, Greece.